POLITECNICO DI MILANO

School of Industrial and Information Engineering

Master of Science in Telecommunication Engineering

POLITECNICO
MILANO 1863

INVESTIGATING THE IMPACT OF RAIN ON D-BAND BACKHAUL LINKS: DATA AND MODELLING

Supervisor: **Prof. Lorenzo Luini**

Master Graduation

Thesis by **Daniel Toribio**

Student ID. Number

905462

Academic Year 2020/2021

Dedication

I want to dedicate this thesis to my parents Gladys Baldeon and Armando Toribio, all my family, my girlfriend and friends, because without their support I would not be here, so I thanks them from all my heart.

I am also thankful for the knowledge I received from all my professors, those from Peru and from Italy, especially by professors Liliana Gagliano, Gabriella Gagliano, Claudio Prati, Angelo Gulinatti, Luca Reggiani, Carlo Riva and Lorenzo Luini.

.

Introduction

The continuous increase in the data rates of mobile communication networks is pushing to explore new frequency bands for backhaul links, such as the D-band (110 to 170 GHz), which can guarantee the larger bandwidth necessary to accommodate the higher capacity. Unfortunately, the detrimental effects that the atmosphere induces on electromagnetic waves increase more and more with the frequency, especially those associated to rain: rain drops, whose dimension is comparable to that of the wavelength in the D band, cause scattering and absorption of the incident electromagnetic energy, which both concur to producing the attenuation of the transmitted signal. The impact of precipitation on backhaul links becomes more and more difficult to estimate as the frequency increases, due to the significant dependence of the specific attenuation on the shape and dimension of the drops. Unfortunately, no experimental propagation data exist for links operating at frequencies in the D-band, nor statistical prediction models that can be used to design such high frequency backhaul links. Originating from a collaboration between Politecnico di Milano and the Huawei European Microwave Centre in Milan, the research activity aims at filling this gap by investigating the effect of rain on a D-band terrestrial link installed by Huawei in the main campus of the university. The link, which is 325-meter long, connects two buildings of Politecnico di Milano and it operates using two different 250-MHz channels, with carrier frequencies 148 GHz and 156 GHz, called respectively Low and High. The research activity will take advantage of the collected data by a collocated disdrometer, which measures the rain intensity. A key goal of the work is to collect a significant amount of rain attenuation data which will be used to optimise an analytical rain attenuation model suitable for the design

of short D-band (which can be used also for E-band) terrestrial links that will be integrated in 5G mobile networks.

Acronyms

EM	Electromagnetic wave
ITU	International Telecommunication Union - Radiocommunication Sector
$M-QAM$	M-level Quadrature Amplitude Modulation
$QPSK$	Quadrature Phase Shift Keying
RF	Radio Frequency
RX	Receiver
TX	Transmitter
UTC	Coordinated Universal Time
SNR	Signal-to-noise-ratio
O_2	Oxygen
H_20	Water
r	Path reduction factor
d	Path of the link propagation
d_{eff}	Effective distance
PRX	Received signal power
PRX'	Interpolated received signal power
PRX''	Filtered interpolating received signal power

A_D	Correction factor
A_R	Rain attenuation
A_T	Tropospheric attenuation
A_G	Gas attenuation
A_{WA}	Wet antenna attenuation
A_{OX}	Oxygen attenuation
A_{WV}	Water vapour attenuation
$CCDF$	Complementary cumulative distribution function
A'_R	Rain attenuation after the removing of the wet antenna
γ_R	Specific attenuation
$\overline{A'(p)_R^{ITU-local-input}}$	Estimation of the rain attenuation made with ITU model by using the local input
$\overline{A'(p)_R^{ITU-derived-input}}$	Estimation of the rain attenuation made with ITU model with derived input
$\overline{A'(p)_R^{Lin}}$	Estimation of the rain attenuation made with Lin's model
$\overline{A'(p)_R^{Opt\ Lin}}$	Estimation of the rain attenuation made with optimised Lin's model.
f	Frequency

P_0	Percentage at 0%
R	Rain rate
P	Probability
$A_R(P)$	Reference attenuation from measurements done at link
$A_P(P)$	Estimated attenuation
GA	Genetic algorithm
LB	Low boundary for GA
UB	Up boundary for GA
m, n	Coefficients for Lin's model and optimised Lin's model

Table of contents

Table of figures

List of tables

Basics

Troposphere

The troposphere is the lowest layer of the atmosphere; there in fact, occurs any meteorological phenomenon, even the formation of clouds. It is characterised by a relationship between height and temperature, as it increases in altitude, it decreases in temperature. Moreover the height will depend on the position on Earth, the upper limit of troposphere, at poles, is around 8 to 10 [km] and at equator is around 18 [km] (see figure 0-1), in addition the height will depend on the season, geographical latitude and meteorological condition.

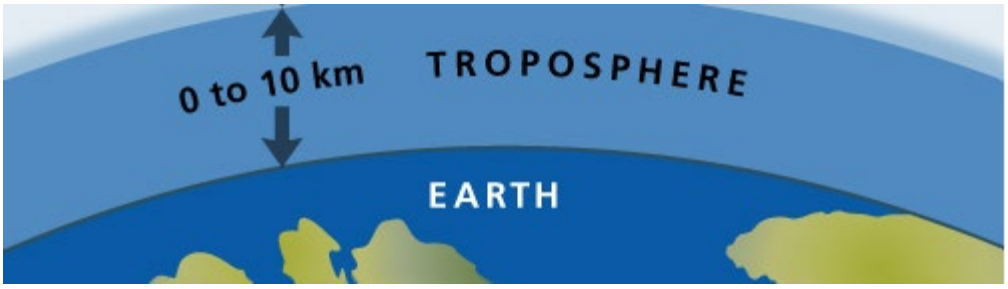

Figure 0-1 The troposphere

Evaporation

it is the process in which the liquid water changes into water vapour because of the heat of terrain, lakes, and river, produced by the solar radiation. In this way water becomes water vapour that rises into the atmosphere.

Condensation

It is a process in which the water vapour, in the air, changes into liquid water, in fact this is the opposite process of the evaporation. Moreover, the formation of clouds and ground-level-fog needs the condensation phenomenon.

ITU

ITU (International Telecommunication Union) is a specialised International organization belonging to United Union which has as objective the responsibility of all regard to Information and communication technology, it means, they develop standards, allocate globally radio spectrum and satellite orbits and improve the ICT (Information communication technology) to be reachable to everyone (ITU, 2020).

ITU-R

International Telecommunication Union – Radiocommunication is a sector of the ITU which exclusively develop standards on radio communication and manages the radio frequency spectrum and satellite orbits. (ITU-R, 2020)

ITU-R 530-17

It is a recommendation method for the design of terrestrial links in clear air and rainfall conditions. This recommendation takes into account the different propagation effects, diffraction fading due to obstruction by terrain, attenuation due to gases, fading due to atmospheric multipath, fading due to multipath from surface reflection, attenuation due to precipitation, variation of the angle of arrival at the receiver, reduction of cross–polarisation

discrimination (XPD) in multipath and signal distortion due to frequency selective media.

Moreover, it recommends two particularly cases, in which it is possible to apply 2 types of inputs: one of them with local inputs and the other one with derived inputs from ITU, which is a fixed value for R(0.01%)=35.3[mm/h] (for the case of this thesis) derived from the ITU-R P.837-7. (ITU-R P.530-17, 2017) (ITU-R P.837-7, 2017)

ITU-R P.837-7

In the possible absence of local input rain rate for the prediction of rain attenuation, the recommendation gives an alternative way to obtain global rain rate statistics. (ITU-R P.837-7, 2017)

ITU-R 838-3

It recommends the use of specific attenuation model, which can be calculated by making use of the rain rate as main parameter.

This thesis will take this recommendation as the basis of further calculation, elaboration, estimation, and optimisation.

The main consideration lies in the need of the rain rate values to calculate the rain attenuation; thus, it recommends the following power–Law relationship

$$\gamma_R = kR^{\alpha}$$

With:

- R: rain rate
- k and α are constant values

Both constants are values depending on the following parameters:

- Inclination of the linear polarization τ, measured in [rad]
- Elevation angle of the antenna θ, measured in radians [rad]
- Operational frequency, measured in [GHz]

(ITU-R P.838-3, 2005)

CHAPTER 1 Tropospheric Effects on Terrestrial Link at High Frequencies

The knowledge of the atmosphere and its effects are important in telecommunication systems for developing more accurate models and results at higher frequencies demanded by new technologies.

An important parameter, which is the source of many observations, is the refraction index, which depends on:

- The frequency of the electromagnetic wave
- Number of electrons in the particle
- Natural frequency of the electrons
- Damping factors

the refraction index as a complex number has the following characteristics:

- From the real component:
  It affects the following phenomena: ray bending, reflection, refraction, multipath, ducting, beam focusing/de-focusing and depolarization.
- The imaginary component:
  It is related to the absorption effects.

1.1 Tropospheric attenuation

Despite all the known benefit of using micro and millimetre waves, it is necessary to know what are the disadvantages of using such waves; specially,

when it travels through in the troposphere, the attenuation affects the signal, which is caused by gaseous absorption and particularly by rain.

In clear tropospheric scenario, the attenuation is due to the absorption by particles of oxygen (O2) and water vapour (H2O) otherwise the rainfall is the main responsible of the signal degradation.

1.2 Gas absorption

As explained above, oxygen and water vapour are the main cause of the attenuation due to molecular absorption at centimetre and millimetre waves.

When the electromagnetic wave impacts on the gaseous polar molecule, which has a dipole moment, it verifies a transfer of energy from incident radiation to the molecule, it means that the molecule gets excited and owns a high energy level, afterwards, the molecule has a change of state, from fully excited state to a decayed state produced by the emission of energy level by the same molecule.

Hence, when there is an interaction between a gaseous molecule and an incident electromagnetic wave two phenomena emerge, the absorption, and the emission of energy by means of the electric and the magnetic pole.

Regarding water vapour, it has an asymmetric top molecule and a permanent electric dipole moment, which produces a rotational energy caused by the rotation of the molecule on different axis. Other kinds of absorption of the energy is produced by:

- the electron energy level, which produces transfer of electrons on the different orbits to the highest energy level
- vibrational energy produced by vibration modes

- the translational energy (or kinetic energy) which can be considered negligible at molecular energy level.

Regarding oxygen, it has a permanent magnetic dipole, it means that only the magnetic field of the electromagnetic wave, interacts with this magnetic dipole, causing absorption.

Then, the calculation of the detrimental effects due to gases must be done by the quantification of the specific attenuation γ_G (dB/km) and the total path attenuation due to gas $A_G = \gamma_G * L$. The result has been done based on the Liebe MPM93 model (Dr. Lorenzo Luini, 2018): see the figure 1-1 :

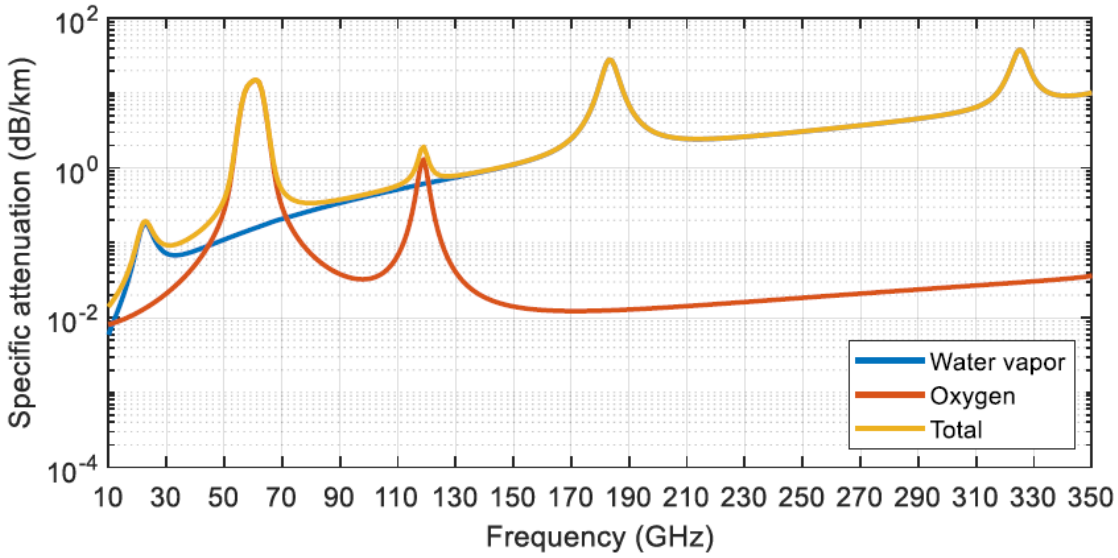

Figure 1-1Frequency spectrum of the specific attenuation due to gases, calculated using the Liebe MPM93 model

The figure 1-1 depicts the general behaviour of the specific attenuation for both elements as a function of the frequency and as it is possible to see, water vapour and oxygen can influence the electromagnetic wave at frequencies between 10 up to 350 [GHz].

Oxygen has an important contribution to specifics frequencies like 60[GHz] and around 120[GHz], instead for water vapour at frequencies around 180[GHz].

This study works at frequencies 148[GHz] and 156 [GHz], part of the D-band, so, the transmission signal will not be so affected by the oxygen and neither significantly by water vapour. However, they are considered in the calculations.

1.3 Tropospheric Scintillation

The scintillation is a physical phenomenon that generates random fluctuation on the amplitude, phase and angle of arrival on the received signal, produced by the turbulence irregularities of the refractive index caused by the pockets of air with slightly different temperatures. In fact, the wave front becomes deflected in many portions. Moreover, it gives rise to interference between those deflected portions and can even destroy the flat phase front of the beam. In addition, this phenomenon is always present in any line-of-sight link at microwaves and further, and can be more intense when rain is present on the propagation path. (John F.Federici, 2016) (Brussaard, 2013) (H. Vasseur, 1995) (John F.Federici, 2016) (T.V Omotosho) (Cheffena, 2010)

1.4 Hydrometeor effects

In a radio link many hydrometeors can have a strong impact on the quality of the signal; those are the following:

- Rain
- Hail
- Wet snow

- Cloud and fog particles
- Snow
- Melting layer particles

The hydrometeors that must be considered depend on the kind of communication link. For example, for an Earth-satellite communication link one must take into account not only the rain but also the clouds, melting layer and so on, in fact, it needs to pass through the whole atmosphere. Another example can be seen from the cloud attenuation, that for frequencies above the 10[GHz] and low elevation angle, can have a significant contribution when there exists a low availability, in this way, the cloud attenuation contributes to defining the link margin. Fog, which consists of suspended water droplets, has as well an impact on the EM wave which cause absorption and scattering, like rain. As it is observed and explained above, the considered parameters will depend also on the type of desired communication.

This thesis deals with rain, as main hydrometeor attenuator, on a terrestrial communication link, as consequence, the other components will not be considered. As cited above, rain is the dominant hydrometeors which affects the electromagnetic field by means of scattering and of absorption at all frequencies. In addition, it becomes relevant for frequencies above the 10[GHz] and, the attenuation increases when the frequencies grow also up to 100 or 200 [GHz]; beyond those values, the specific attenuation decreases, as observed in the figure 1-2 (Brussaard, 2013)

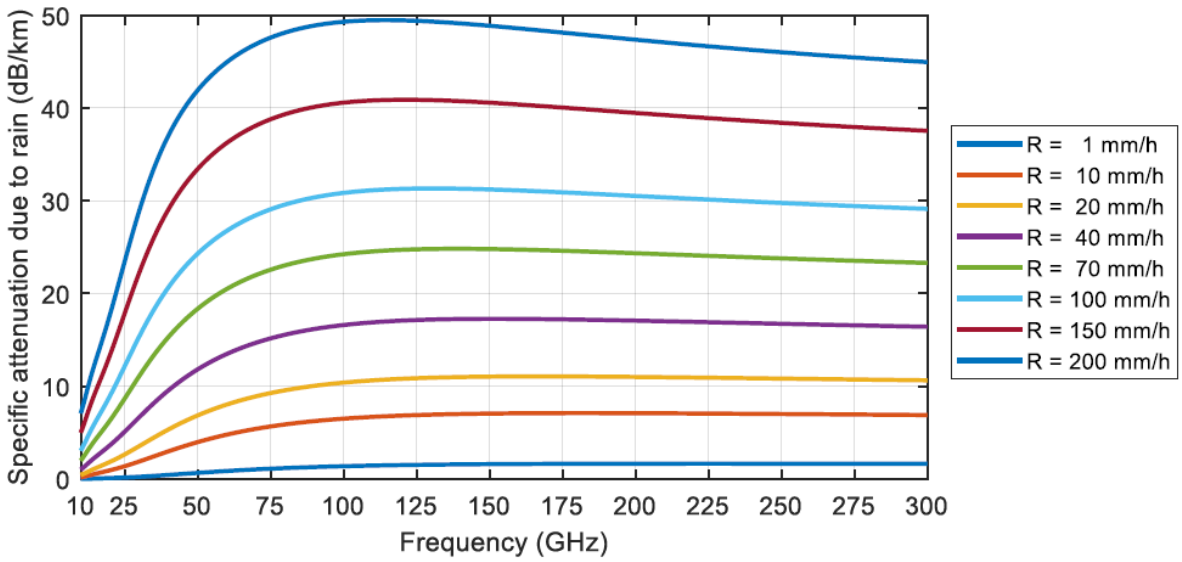

Figure 1-2 Trend of specific attenuation due to rain with frequency, for different rain rates, calculated according to recommendation ITU-R P.838-3

Theoretical and experimentally studies confirm that wavelength, between the 30[mm] and 1.5 [mm], are subject to attenuation caused by the comparable diameter of drop and the wavelength, typically around 1[mm] and 1.5[mm]. (Brussaard, 2013)

1.4.1 Precipitation

Considering that the tiny condensed particles grow, produced by the collision or fusion, the gravity force which push them down and that the raising air will no longer sufficient to support them, what happens is that, the condensation particles fall down to the Earth in form of Rain , Hail, Snow and Sleet.

This thesis will take only into account on the Rainfall Precipitation

a. Rainfall precipitation

It is a liquid water in form of droplets that have been condensed from the atmospheric water vapour and become heavy enough to fall down because of the gravity.

The raindrop will vibrate, oscillate, and become deformed while it is falling due to the gravity and the wind.

b. Shape of the raindrop

The raindrop shape is typically illustrated as a teardrop but, actually, the real shape will depend on its dimension and on the falling speed through the atmosphere. See figure 1-3 and 1-4.

In fact

- the drop that has a radius less than 1 millimetre [mm] has a spherical shape, because of the surface tension which is stronger than in larger drops and it is the consequence of air flow around the drop. The more the raindrop falls, the more its spherical shape will change.
- For a radius greater than 1 [mm], the shape begins to be oblate but flat on the bottom. It happens because of the speed falling through the atmosphere.
- When the raindrop becomes bigger, because of the collision or fusion with other drops, the radius will be about 4.5 [mm], and it gets separated like a parachute, see figure 1-3 and 1-4.

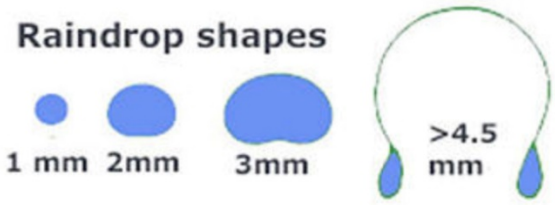

Figure 1-3 Falling raindrop shape

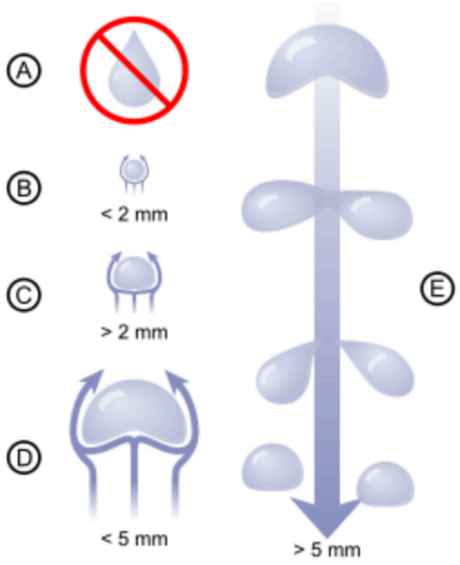

Figure 1-4 Falling raindrop shape

(NASA, 2020) (Fraser, 2020)

c. Types of precipitation

c.1 Convective Event

It occurs when a specific and limited terrain becomes hot so much that all the water evaporates; in this way, the vertically air rises the water vapour and generates convective clouds, which are limited vertical and horizontally, and convective rain. See figure 1-5.

A particular characteristic of this kind of event is that the precipitation falls over a specific area with high intensity and short duration. It is typical of summer showers and of tropical regions like the Amazons.

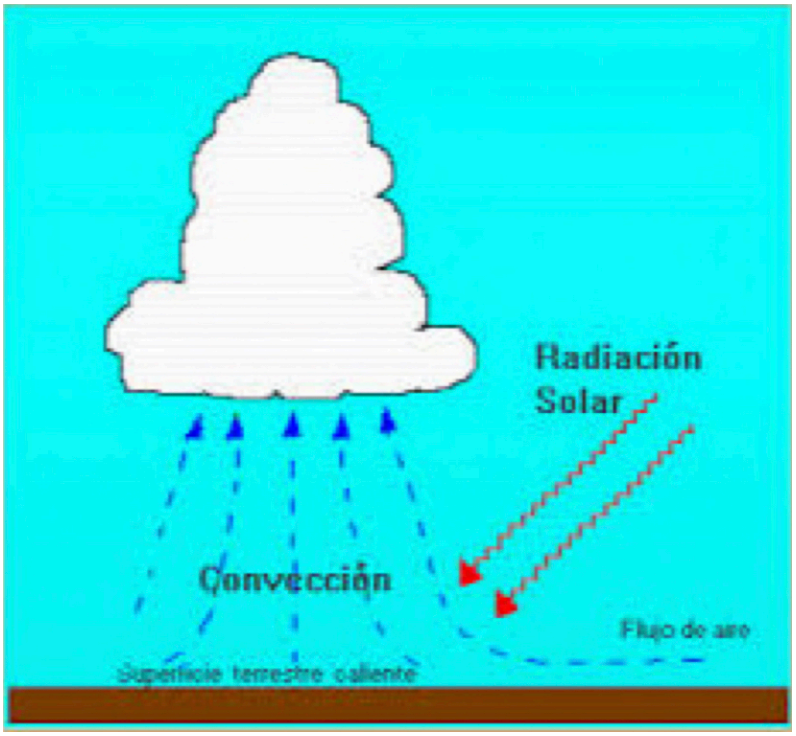

Figure 1-5 convective precipitation

c.2 Stratiform Event

It is characterised by an extended horizontal cloud which is formed by the water vapour pushed diagonally up from the air.

The precipitation is uniform and less variable in space and time, in addition, it has a low rain intensity and the rain can reach the height of the Bright Band, consisting of water-coated snow flakes.

Other kinds of precipitation exist, like: Moonsoon precipitation, it is a combination of convective and stratiform; in fact, it has many bands of intense convection and intervals of stratiform precipitation, it is characterized by heavy precipitation for several hours; the tropical storm, it is a kind of

precipitation which extends for hundreds of kilometres. It is characterized by several spiral bands and each band has a region of intense convection. (Brussaard, 2013)

d. Rain accumulation

It indicates the falling quantity of rainwater over a flat, horizontal, and impermeable surface. It is measured in [mm] (millimetres of rainfall).

To keep in mind:

- Measure unit: $[mm]$
- $1[mm] = 1[L/m^2]$ $(litre\ over\ squared\ meter)$
- $1[m^3](cubemetre) = 1000\ [L]$

e. Rain rate

It is defined as the rain accumulation measured over a given time unit. It gives information about the intensity of the rain precipitation in any moment, so the instantly precipitation.

- The measured unit is : $[mm/h]\ millimetres\ of\ water\ in\ 1\ hour$

(Ombra, 2014)

By resuming the 1.4.1, see table 1-1:

Table 1-1 Definition, impact and use of rain rate

Definition	Quantity of water fell on a surface in an interval of time
Unit of measure	[mm/h]
Impact on EM wave	Dominant contributor of attenuation

Collected data	Disdrometer
Extraction data	Ad-hoc MATLAB script: "EXTRACT_RAINRATE.m"
Useful data for	• Optimising the synchronization of the received power. • Detecting the rainy events of the any day. • Calculating the rain attenuation. • Estimating the rain attenuation.

1.4.3 Rain Attenuation

Rain, as explained above, is the principal contributor of fading. Its impact on the EM wave, at higher frequencies, especially above the 10 [GHz], will depend particularly by the size of drop. In fact, when the wavelength and the dimension of drop are comparable in size, the EM wave suffers from a detrimental effect caused by absorption and scattering.

a. Absorption and Scattering from drops

The scattering and absorption phenomena are produced for wavelengths in the range of $30\ [mm]$ to $1.5\ [mm]$ regard to drop size around $1[mm]$ and $6[mm]$ (Brussaard, 2013), in this case, where there exist this comparison, the following expression is applied to determine the specific attenuation:

$$\gamma_{\mathrm{R}} = 0.434.10^{3} \int_{\mathrm{D}} \sigma_{\mathrm{ext}}(\mathrm{D})\,.\,\mathrm{N}(\mathrm{D})\ \ \mathrm{dD} = \left[\frac{\mathrm{dB}}{\mathrm{Km}}\right]$$

Where:

- $D(\sigma_{ext})$: Rain drop with a given diameter, with number of rain drops with the same size.
- $\mathrm{N}(\mathrm{D})$: Drop size distribution (DSD), it denotes the number of rain drop with a specific size contained into $1\ m^3$, it is measured by $\mathrm{mm}^{-1}\mathrm{m}^{-3}$ expressed as below:

$$N(D_i) = \frac{10^6 n_i}{Sv(D_i)T\Delta D_i}(mm^{-1}m^{-3})$$

  - ni : number of raindrops whose diameter falls in the i-th class
  - $\Delta D_i(mm)$: the width of each drop-size class
  - $S(mm^2)$: Disdrometer sampling area
  - $T\ (seconds)$: the instrument integration time

- $v(D_i)$ (m/s) : terminal velocity of rain drops

- σ_{ext}: Total cross-extinction section, defined as an area, which is composed by the σ_{sc} and the σ_{abs}, as follow:

$$\sigma_{ext} = \sigma_{sc} + \sigma_{abs} \quad [m^2]$$

  - The σ_{sc} indicates the area where the total energy flux is scattered by the drop.

$$P_{sc} = \sigma_{sc}\, S \quad [W]$$

    - S: $wave\ power\ density$ $[W/m^2]$

  - The σ_{sc} indicates the absorbed energy by the drop.

$$P_{abs} = \sigma_{abs}\, S \quad [W]$$

So, the total power lost is expressed as follow:

$$P_{att} = \sigma_{ext}\, S \quad [W]$$

The recommendation (ITU-R P.838-3, 2005) after the collection of different rain rate data, achieves to the accurate expression of the specific attenuation,

$$\gamma_R = kR^{\alpha} = \left[\frac{dB}{Km}\right]$$

whose behaviour can be observed at different frequencies and different rain rate data, as shown in figure 1-2

This thesis does not consider the depolarization due to the short link distance.

CHAPTER 2 Experimental equipment and data

2.1 Terrestrial link operating at D-band

The experiment, realised within the collaboration of Huawei European Microwave Centre in Milan and Politecnico di Milano, has been installed on the top of roofs of building 20 (DEIB) and 14 (La Nave). The link has a distance of 325 meters operate at D-band, see figure 2-1, whose band goes from 140[GHz] to 160[GHz]; for this specific study, two carriers will be considered: one at 148[GHz] and the other one at 156[GHz], denominated “Low” and “High”, respectively, and each of them has a channel bandwidth of 250[MHz].

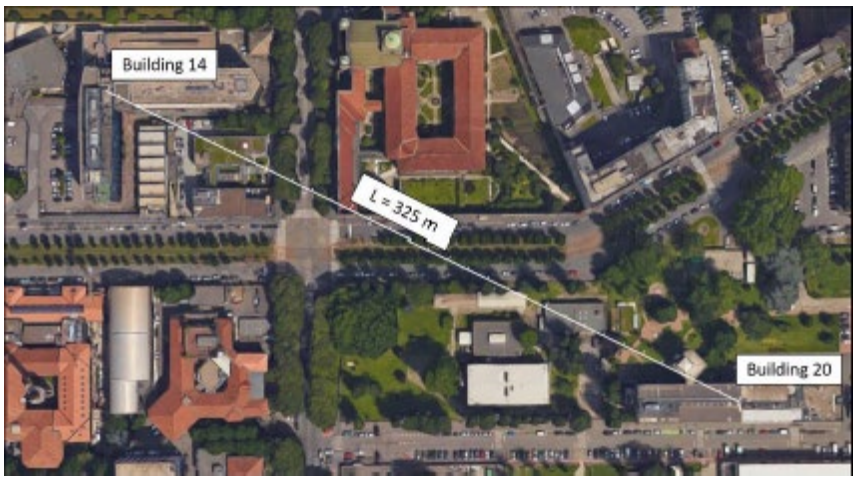

Figure 2-1 Path of Huawei links connecting Buildings 14 and 20 of Politecnico di Milano

The antennas are positioned at 1 meter from the surface of the building’s roof, see figure 2-2, in order to guarantee that the first Fresnel’s ellipsoid is free and avoid reflected waves that could impact the propagation link. In addition, the antennas have a gain around 34 dBi and the wave is horizontally polarised.

Figure 2-2 Huawei E-band and D-band transceivers installed on the rooftop of Building 20 of Politecnico di Milano.

The equipment has an atmospheric fade margin of 15 dB.

Moreover, the system operates with QPSK (Quadrature Phase Shift keying) modulation in order to increase the signal-to-noise-ratio (SNR), but it can work also with M-QAM.

To resume, see table 2-1:

Table 2-1 System parameters of the D-band link

	D-band
Bandwidth	250 MHz
Transmitter power	+5dBm
Receiver sensitivity	-67dBm with QPSK
Antenna gain	34 dBi
System gain	140 dB
Wave polarisation	Linear vertical
Carrier Frequencies used	148 GHz (Low) 156 GHz (High)

Atmospheric fade margin	15 dB

The collected data are transferred through an Ethernet cable and saved onto a computer in the DEIB department.

2.2 Disdrometer

Another instrument, used in this experiment, is the Disdrometer, see figure 2-4, which is a laser-based device that emits a beam, whose wavelength is $785[nm]$ (near-infrared region) over a surface equal to $4560[m^2]$ and has a Height of $0.75[mm]$, as can be observed in figure 2-3:

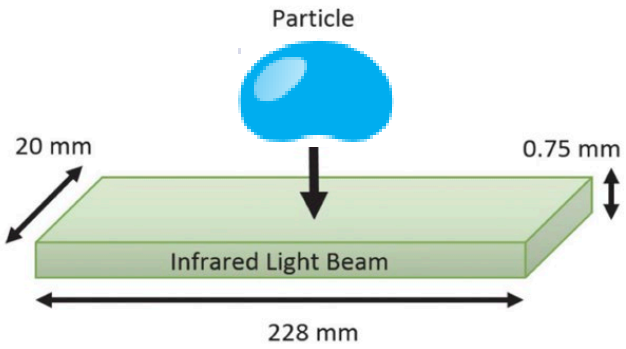

Figure 2-3Diagram depicting the disdrometer measurement of a precipitating particle

When the hydrometeors cross the beam, they cause an interruption of the transmission allowing the Disdrometer to detect different parameters of the hydrometeor; in fact, it can individuate the falling velocity, the dimension, the drop shape (within an Interval between 0.125 to 8[mm]); in addition, this device can also classify the crossing object like a rain , snow or hail.

Furthermore, the Disdrometer can measure the rain rate, which will allow to determine the quantity of rainwater fall at a specific time.

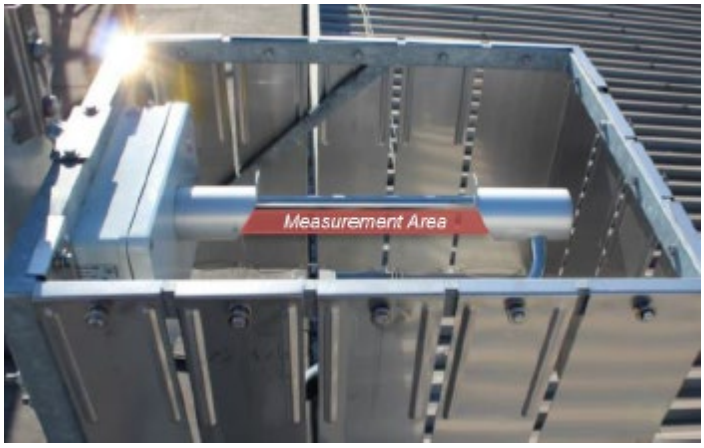

Figure 2-4 Disdrometer installed on the rooftop of Building 20 – Politecnico di Milano campus

2.2.1 Data and Sampling

The transceiver equipment is operative since February 2017, but it was interrupted in February 2018 due to the insertion of a hydrophobic protection around the antennas in order to guarantee a higher accuracy. This is the reason why this thesis will deal with data collected in the period February 2018- February 2019. In additional, momentary problems to the equipment (e.g. blackouts) causes lack of data in specific days.

Data are collected with 3-second sampling time and they are saved in a CSV file.

CHAPTER 3 Extraction and Elaboration of Data

3.1 Extraction of the Received Signal Power

Two programs were created for extracting row data; the first one, called SEQUENCE, extracts and elaborates, uninterruptedly, the available CSV-files, with just setting the beginning desired date (it will work for D-band-High and D-band-Low values).

The second program, called CLASSIC&COMBINED extracts and elaborates specific/different desired dates belonging to a specific year.

3.1.1 Pre-configuration and Configuration of the Programs

a. Pre-configuration

a.1 Classification of CSV-files

Before running any program, the CSV-files must be classified manually, for both cases, “High” and “Low”, hence, it is advisable to create a dedicated folder, named for example “D_band_2018”, which will contain only the high and low CSV-files associated to that specific year and band. The same procedure must be applied to other years and bands.

a.2 Rain rate files

The precipitation data comes from the disdrometer and are extracted and elaborated by the ad-hoc MATLAB script, named “EXTRACT_RAINRATE.m”. It produces rain rate files in mat-format, which are ready to use into the main programs SEQUENCE or CLASSIC&COMBINED.

The rain rate files contain information regarding daily precipitation averaged to the minute expressed in [mm/h], those files are useful , initially, to do a quickly comparison with the result obtained from the received signal power PRX, in order to observe if the behaviour of the rain rate is synchronized with the receive signal power related to the same date, i.e. if the top peaks of the rain rate corresponds with the bottom peaks of PRX; it is also useful to identify the rainy events and mainly for calculating the specific attenuation and rain attenuation.

b. Configuration

Once it is pre-configurated, then, it is necessary to open the main script and setup what is desired to elaborate.

b.1 Sequence Program case:

b.1.1 Addresses

It must be:

CSV address

- Define the address of the folder where the CSV-files are saved, by taking into account the previous example, the address of the folder "D_band_2018" must be put onto the dedicated space in the script.

Saving address

- Define the name of the folder where all elaborated files will be saved, for example, "Results_2018"
- Define the address where the new folder "Resulsts_2018" will be created.

Rain Rate address (1): Full dates

- Define the address of the elaborated rain rate files, in mat-format, and put it into the dedicated space. The address will call the whole rain rate files independently if it rains or not, so, if a dry day is selected, the figure will depict a flat graph. See figure 3.1 and 3.2.

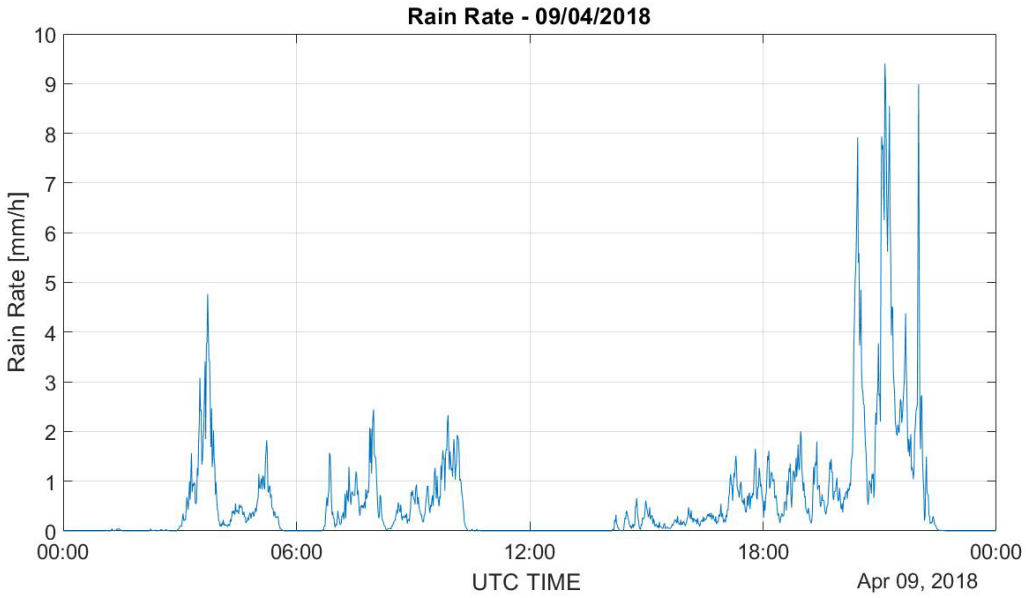

Figure 3-1 Rain rate of a rainy day

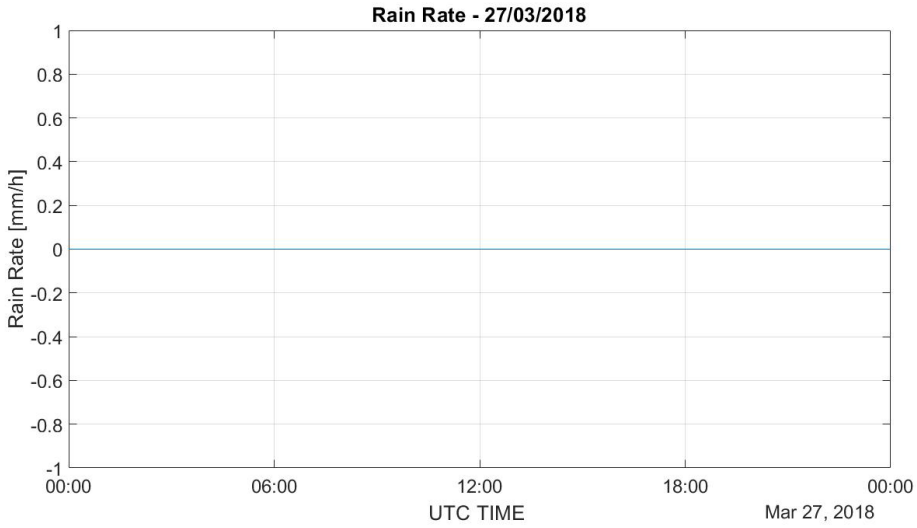

Figure 3-2 Dry day

Rain Rate address (2): Only rainy events

- Define the address of the rain rate files, in mat-format, where only the rainy days (see figure 3-1) are, and put it into the dedicated space.

b.1.2 Characteristics of the desired results

- Define the beginning date in the following format: “dd/mm/yyyy”
- Define the band: “D” (for D-band) or “E” for E-band
- Define the frequency of the carrier: “L” (for Low frequency) or “H” (for High frequency).

b.1.3 Flags

win_rain (window rain)

- “win_rain”, windows rain, is set as “1” if one desires to observe the received signal power together with the rain rate (see figure 3.3); otherwise with “0”, it will only plot the received signal power.

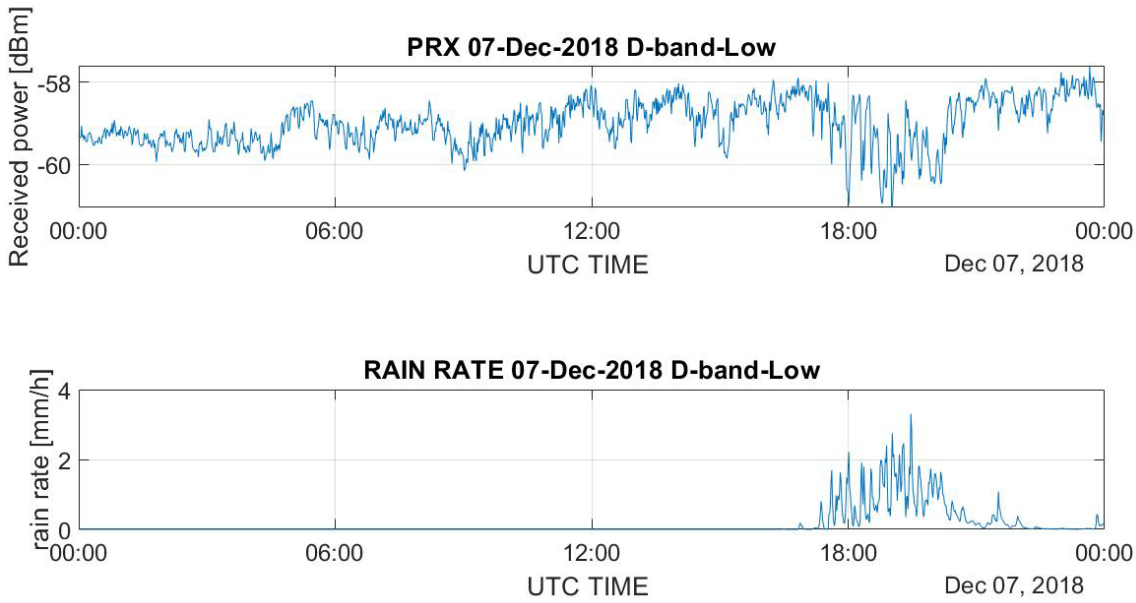

Figure 3-3 Due to flag win_rain set up to 1, the figure depicts the PRX and rain rate

Sync (forcing synchronization)

- When "sync" is set to "1", the rain rate and PRX time series will be synchronized; the criteria is based on the comparison between top peaks of the rain rate and the bottom peaks of the received signal power. The sync function shifts the receive signal power of some minutes until the best agreement between peaks is found.

b.2 CLASSIC&COMBINED CASE:

b.2.1 Addresses

It must be:

CSV address

- Define the address of the folder where the CSV-files are saved, by taking into account the previous example, the address of the folder "D_band_2018" must be put onto the dedicated space in the script.

Saving Address

- Define the name of the folder where all elaborated files will be saved, for example, “Results_2018”
- Define the address where the new folder “Resulsts_2018” will be created.

Rain Rate address (1): Full Dates

- Define the address of the elaborated rain rate files, in mat-format, and put it into the dedicated space. The address will call the whole rain rate files independently if it rains or not, so, a dry day is selected, the figure depicts a flat graph. See figure 3-1 and 3-2.

Rain Rate address (2): Rainy Events

- Define the address of the rain rate files, in mat-format, where only rainy days are (see figure 3-1) and put it into the dedicated space.

b.2.2 Characteristics of the desired results

- Specify, onto the dedicated space, the single desired date, defined as ‘dd/mm/yyyy’ ; on the other hand, for many dates belonging to the same year, they must be separated by a comma, as in the following example: '13/05/2020','14/05/2020','15/05/2020'.
- Define the band: “D” (for D-band) or “E” (for E-band).
- Define the frequency of the carrier: “L” (for Low frequency) or “H” (for High frequency).

b.2.3 Flags

win_rain (windows rain)

"win_rain", windows rain, is set to "1" to observe the received signal power together with the rain rate (see figure 3.3), otherwise with "0", it will only plot the received signal power.

Sync (forcing synchronization)

- When "sync" is set to "1", the rain rate and PRX time series will be synchronized; the criteria is based on the comparison between top peaks of the rain rate and the bottom peaks of the received signal power. The sync function shifts the receive signal power of some minutes until the best agreement between peaks is found.
- "Manual_sync" is set to "1" to impose a determined number of minutes to shift. It can be used in case the delay number of minutes belonging to a single determine date is known; in this way the received signal power must be shifted by the imposed number of minutes and match with the rain rate, otherwise it is set to "0"

After the pre-configuration, configuration and running, the results, regarding a single date, will contain 1440 samples related to 1 minute per sample: all the data are averaged over one minute, as this is the integration time of the disdromter data.

3.2 Synchronization of data

The criteria used to elaborate the received signal power of a single date is based on the research of all the available CSV-files which contain all the data associated to a specific date.

From each CSV-file, the script will extract two pieces of information that will help synchronize the samples. The first one is the sampling time beginning, which can be derived from the name of the CSV-file; the second one is the last second of data sampling: this is extracted from the "last modified" date of the same CSV-file.

In this way, date and time can be fixed, by having as reference, the UTC time (Universal Time Coordination). The sampled data are associated to the Italian time zone; hence, the time stamp need to be adapted as follows:

- In case of Italian summertime, there is a +2 hour shift from the UTC time. The summertime begins on the last Sunday of March at 01:00 UTC (02:00 AM in Italy) and ends on the last Sunday of October at 01:00 UTC (03:00 AM in Italy).
- The winter time is shifted by +1 Hour from the UTC time. The wintertime begins on the last Sunday of October at 01:00 UTC time (at 03:00 AM in Italy) and ends on the last Sunday of March at 01:00 UTC (02:00 AM). (RecensioniOrologi, 2020)

Thus, the correction in time will be done by taking into account the above considerations.

For example:

- For winter time: The date 24/02/18 15:15:15 (Italian time) will be corrected as 24/02/18 **14**:15:15 UTC time.
- For summer time: The date 03/07/18 14:14:14 (Italian time) will be corrected as 03/07/18 **12**:14:14 UTC time.

After applying such a correction to the start and ending time of the sampling file, it is possible to derive the time stamp for each sample by dividing the total time by the number of available samples , i.e. 28800 samples for a full CSV-file.

3.3 Elimination of the outlier

It is the suppression of the atypical samples of the received signal power: occasionally the PRX takes extremely high or low values (spikes) not associated to any rainy event.

The criteria used to write the code is the following:

- It is taken a short fragment of samples from the current CSV-file
- It is calculated the average of the previous taken fragment
- It is considered a short range of PRX by having as reference the calculated average value
- Subsequently, the same taken fragment is read again in order to discriminate samples that overcome the established range

A light version of this code has been also written which is used exclusively during the precipitation time, in this way it is avoiding the suppression of correct samples.

3.4 Attenuation due to Gas

Oxygen and water vapour do not have a heavy impact for the specifically frequencies taken into account in this experiment (148 [GHz] and 156[GHz]),

see figure 1-1; notwithstanding their low impact, they are considered in order to have more accurate results.

- Notice that for any frequency greater than 10[GHz], the gas attenuation must be calculated, see figure 1-1.

The attenuation due to gas has the following expression:

$$A_G = A_{OX} + A_{WV}$$

- A_{ox}: Attenuation due to Oxygen
- A_{wv}: Attenuation due to water vapour
- A_G: Gas attenuation

In case of dry days it is possible to say that the tropospheric attenuation depends only on the gas attenuation, as it can be observed in the following expression:

$$A_T = A_G = A_{OX} + A_{WV}$$

- A_T: Tropospheric attenuation

Otherwise the tropospheric attenuation assumes its complete expression:

$$A_T = A_R + A_G$$

The gas attenuation data are obtained by using the prediction model included in recommendation ITU-R P.676 (Annex 1), which allows calculating the specific attenuation due to gases using as input the pressure, temperature and relative humidity. These data, in turn, are extracted from the University of Wyoming website (Wyoming, University of Wyoming, 2020), which collects meteorological data with 30-minute sampling time from several stations worldwide. For this experiment, the data are associated to the meteorological

observations carried out at Linate airport (5 km of distance from the experimental site), Italy (LIML) (Wyoming, Observations for MILANO LINATE, Italy (LIML), 2020)

3.5 Extraction of the rain attenuation

To obtain the rain attenuation measured along the link, first of all, the PRX must be elaborated.

a. PRX' signal

To obtain the PRX' values, the identification of rainy events is needed.

a.1 Identification of the rainy events

The criteria used to identify the rain events are based on the following steps:

- A rainy event is considered when the precipitation exceeds 0.05 [mm/h].
- An event must contain at least 2 samples (equivalent to 2 minutes).
- An event must be separated to another event by at least 60 minutes in which there is not a precipitation, or the precipitation is lower than 0.05[mm/h]. See figure 3-4.
- Some rain events affect two or more days. See figure 3-4(b)

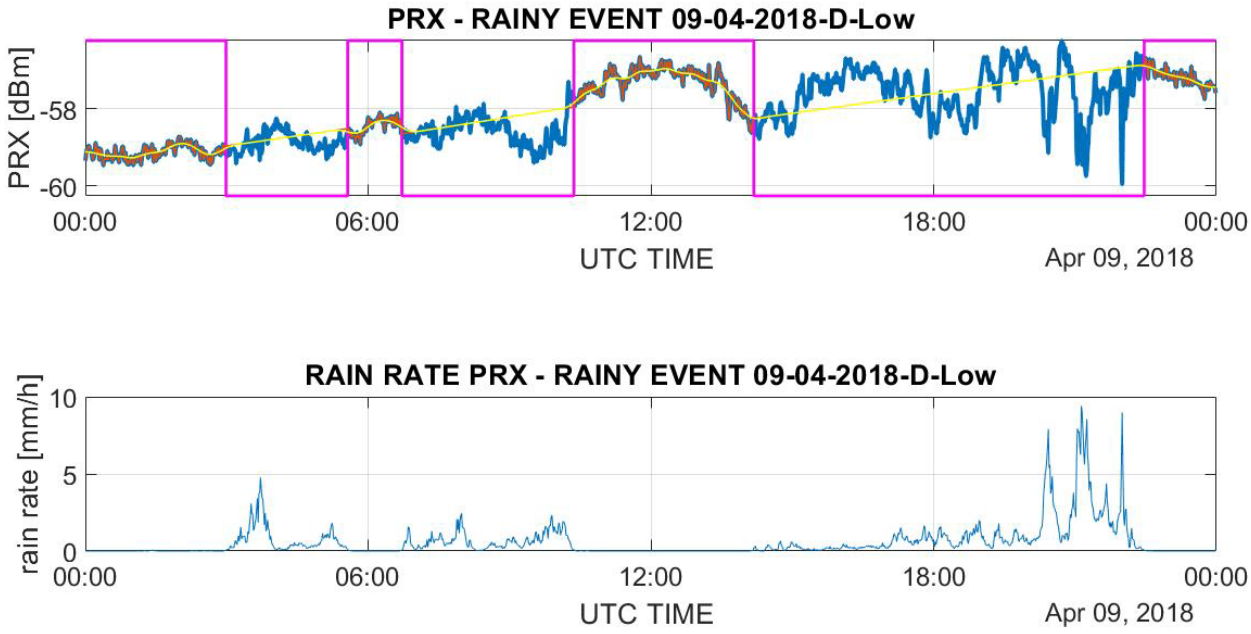

Figure 3-4 (a)

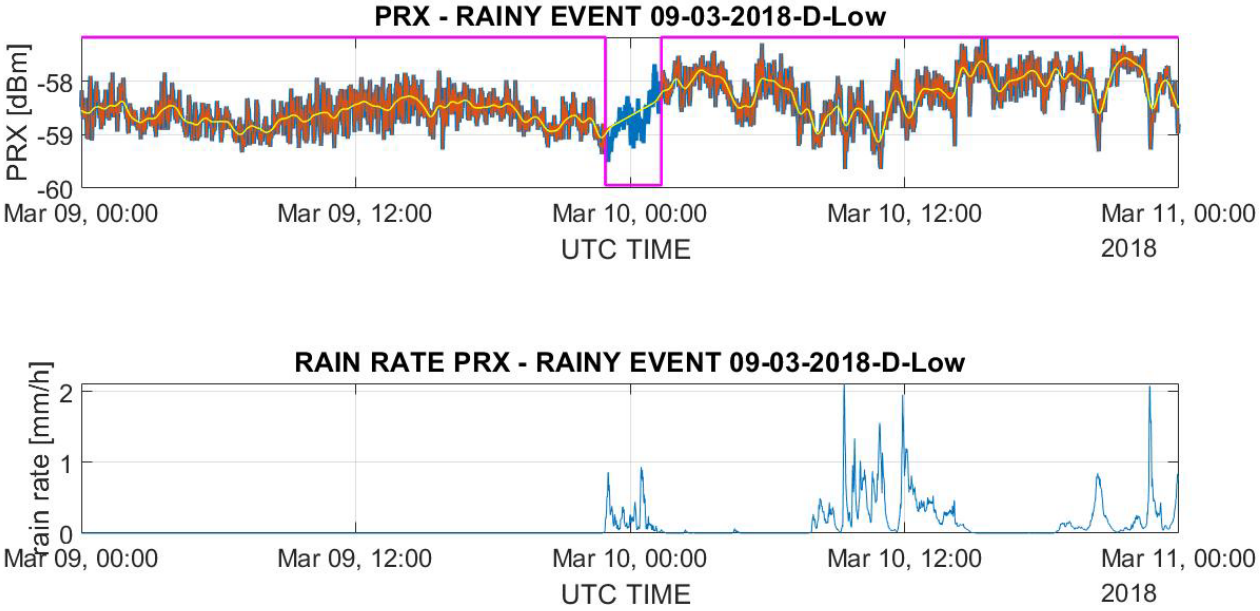

Figure 3-4 (b)

Figure 3-4(a)(top figure) On date 09-04-2018 for D-band-Low, pink curve identifies three rainy events ; (b)(bottom figure) On date 09-03-2018 for D-band-Low can be observed the only rainy event, which is a continuous rain, identified by pink curve, from last hours of date 09th March to some hours of 10th March

a.2 Linear interpolation during rainy events

The next step is the interpolation. Once a rain event is identified, the following steps are taken:

- Identify the PRX sample before to start the rainy event.
- Identify the single PRX sample after the end of the rainy event.
- Apply the interpolation between the two previously identified PRX samples with an interval step equal to 1 minute. See figure 3-5.

Only now it is possible to construct the PRX' signal.

- the new obtained PRX' curve will be composed by two curves: the first one is the same PRX curve but on the temporal range outside of the rainy event and the second curve is that interpolated (during rain events).
- the final vector length of PRX' must have also 1440 samples

By making a zoom on the figure 3-4 is obtained the figure 3-5 and figure 3-6, where it is possible to identify the orange curve, which is behind the yellow curve; it indicates the PRX'', produced by the linear interpolation.

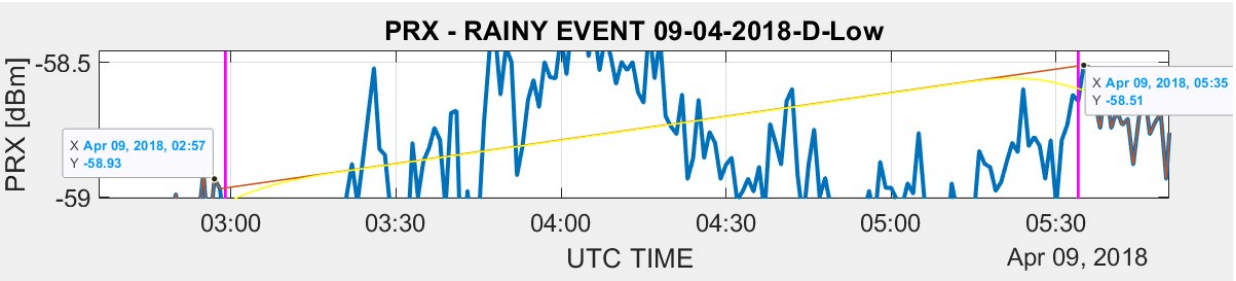

Figure 3-5 Selection of the two external samples from the rainy event for interpolating

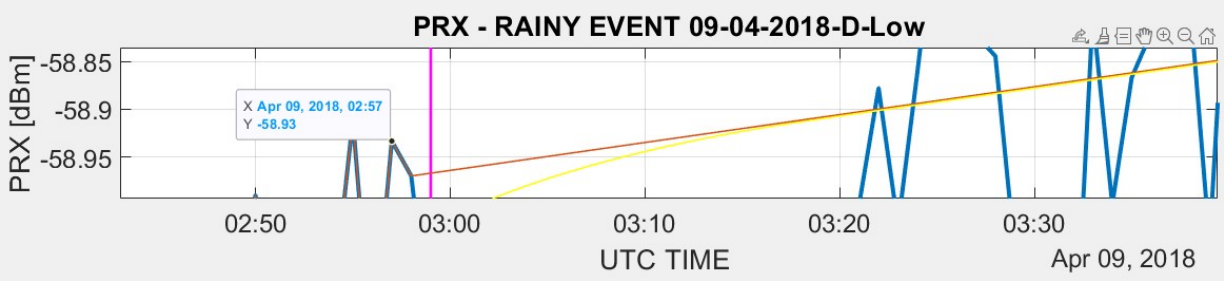

Figure 3-6 Zoom of the date 09-04-2018-D-Low for observing the orange curve which indicates the PRX'' curve done during the rainy event

b. PRX" signal

In case of rain-free condition and absence of fog, the tropospheric attenuation matches with the attenuation due to gases $A_T = A_G = A_{OX} + A_{WV}$, hence, it can serve as reference to determine A_T from PRX and as a consequence obtain the rain attenuation A_R.

Thus, the gas attenuation component (A_G), described in 3.4, is a key parameter to determine the rain attenuation (A_R). Indeed, for the derivation of A_R, we need the gas attenuation, the identification of the rain events and the PRX only associated with the gas attenuation, which is represented by PRX''. The gas attenuation reference is used in rain-free conditions, i.e. when the signal is affected only by gases (PRX''): this is how it is possible to achieve the calculation of the correction factor A_D (as in 3.5.c). Then, the tropospheric attenuation is easy to calculate as in 3.5.d and the rain attenuation can be obtained by subtracting the gas attenuation from the total tropospheric attenuation as in 3.5.e.

b.1 Filter (Low Pass Filter)

It is a low pass filter, which works with a moving average of $cos^2 - shape$ and block length equal to 50. It is used to remove fast oscillations of the signal.

After applying filter the obtained signal is the PRX'' signal. The curve is observable in figure 3.4 in yellow.

c. Correction factor A_D

A_D is a correction factor parameter used to calculate the tropospheric attenuation.

A_D has the following expression:

$$A_D = -P''_{RX} - A_G$$

d. Tropospheric attenuation

It is expressed as follow:

$$A_T = -P_{RX} - A_D$$

e. Rain attenuation

Finally, the attenuation due to rain has the following expression:

$$A_R = A_T - A_G$$

f. Availability

The availability is calculated as the number of available minutes of rain rate (and rain attenuation) values, over the number of minutes of the entire year. It is measured in percentage.

In case of this experiment, the following results have been obtained (table 3-1):

Table 3-1 Availability of D-band on date 5 February 2018 to 5 February 2019

Total D-band: 5Feb2018-5Feb2019	74.20%
Low D-band: 5Feb2018-5Feb2019	74.39%

High D-band: 5Feb2018-5Feb2019	74.01%

CHAPTER 4 Estimation of rain attenuation

The estimation model to be obtained in this thesis aims at predicting the rain attenuation statistics. Specifically, two predictions models are applied, and one of them is optimized to provide better agreement between predictions and measurements.

Thus, in this chapter the rain attenuation statistics measured by the link are compared with the results obtained by the following models:

- ITU Recommendation model 530.17
- Lin's model
- Optimised Lin's model

The results obtained in this model rely not only on the data collected at D-band (148[GHz] and 156[GHz]), but also on those derived at E-band (73[GHz] and 83[GHz]) in (Lorenzo Luini S. M., 2020): in fact, the goal is to obtain a model that can be used on an extended frequency range.

4.1 Statistic Analytics

4.1.1 CCDF (complementary cumulative distribution function)

The CCDF defines the probability that a random variable X is greater or equal to a reference "x" value, i.e. the exceedance probability.

Mathematically it is expressed as follow:

$$F_X(x) = P(X \geq x)$$

a. RAIN RATE CCDF

Before deriving the CCDF of the rain rate, it is necessary to select only those values of rain rate that corresponds to the rain attenuation values collected by the link (as already mentioned, some outage periods are due to blackouts or problems with the experimental equipment).

Figure 4-1 shows the CCDF of the rain rate.

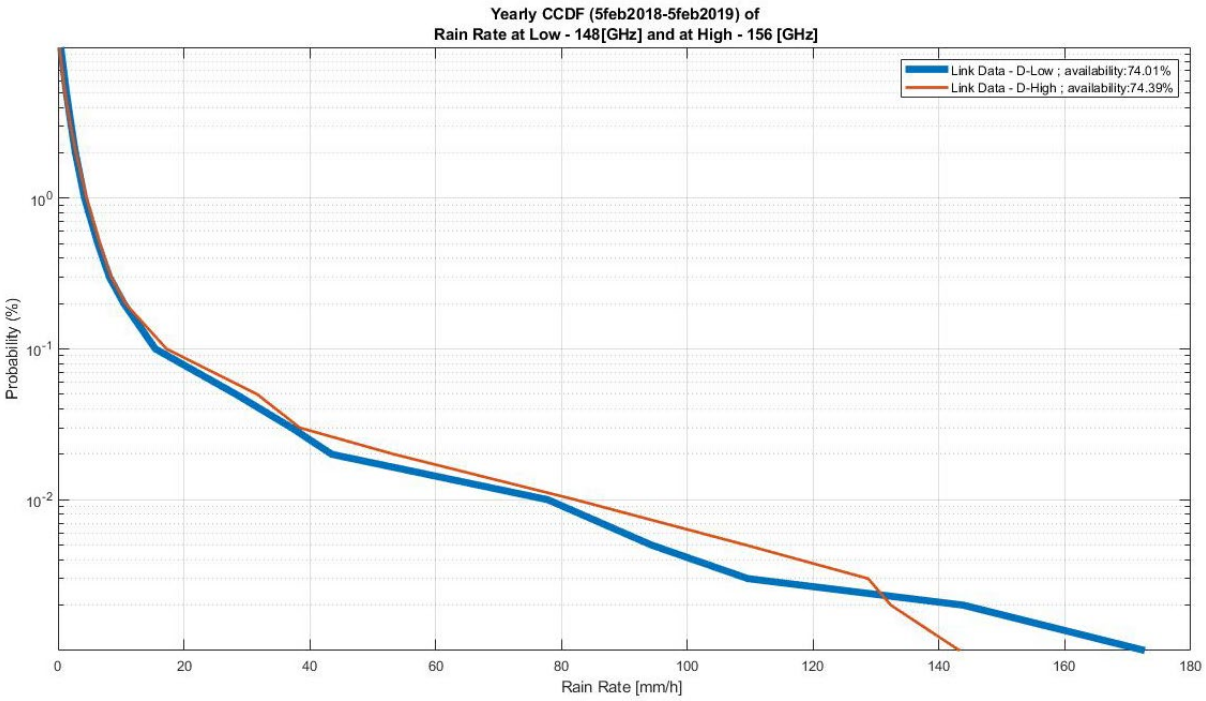

Figure 4-1Yearly (5feb2018-5feb2019) CCDF of RAIN RATE at the frequencies 148[GHz] and 156[GHz] belonging to D-band.

Table 4-1 reports additional information.

Table 4-1 Probability to exceed the rain rate for 0.01% of the yearly time at frequencies 148[GHz](Low) and 156[GHz](High) and probability to have rain, from 05 February 2018 to 5 February 2019.

	D-band-Low (148[GHz])	**D-band-High (156[GHz])**
Probability to have rain	$P_{(R=0.2[mm/h])} = 10.46\%$	$P_{(R=0.2[mm/h])} = 10.30\%$
Rain rate exceeded for 0.01% of yearly time	$R_{0.01\%} = 77.83 \left[\frac{mm}{h}\right]$	$R_{0.01\%} = 82.22 \left[\frac{mm}{h}\right]$

The results for the rain rate CCDF are listed in table 4-2.

Table 4-2 Values of the rain rate CCDF at D-band-low (148 [GHz]) and at D-band-high (156[GHz]) from the period 5 February 2018 to 5 February 2019

R_{low}**(%p) [mm/h]**	172.70	143.84	109.62	94.34	77.83	43.52	37.11	28.28
R_{high}**(%p) [mm/h]**	143.27	132.33	128.73	109.37	82.22	53.43	38.42	31.65
$p(\%)$	0.001	0.002	0.003	0.005	0.01	0.02	0.03	0.05

R_{low}**(%P) [mm/h]**	15.46	10.45	8.16	6.32	4.21	2.75	2.10	1.32	0.43
R_{high}**(%P) [mm/h]**	17.24	10.71	8.43	6.63	4.53	2.84	2.01	1.10	0.22
$p(\%)$	0.1	0.2	0.3	0.5	1	2	3	5	10

b. WET ANTENNA EFFECT

Previous studies (Lorenzo Luini G. R., APRIL 2020) evidence that the permanence of water on antennas after a precipitation event causes an additional attenuation due to antenna being wet, which has an impact on the result of the receive signal power, hence on the estimation of the rain attenuation. The impact of the wet antenna can be observed in figure 4-2, figure 4-3.

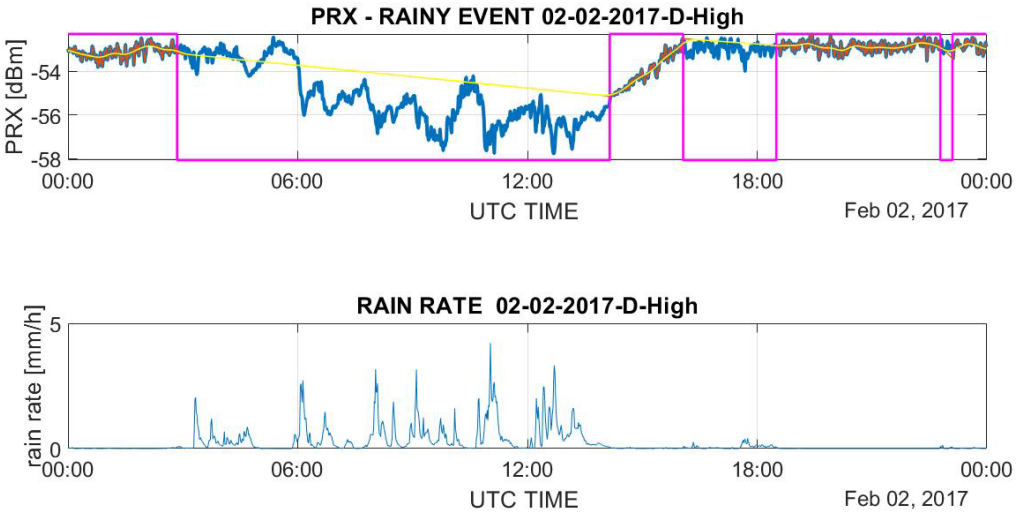

Figure 4-2Wet antenna effect impact on the PRX signal between 14:00 and 16:00. Zoom on in figure 4-3

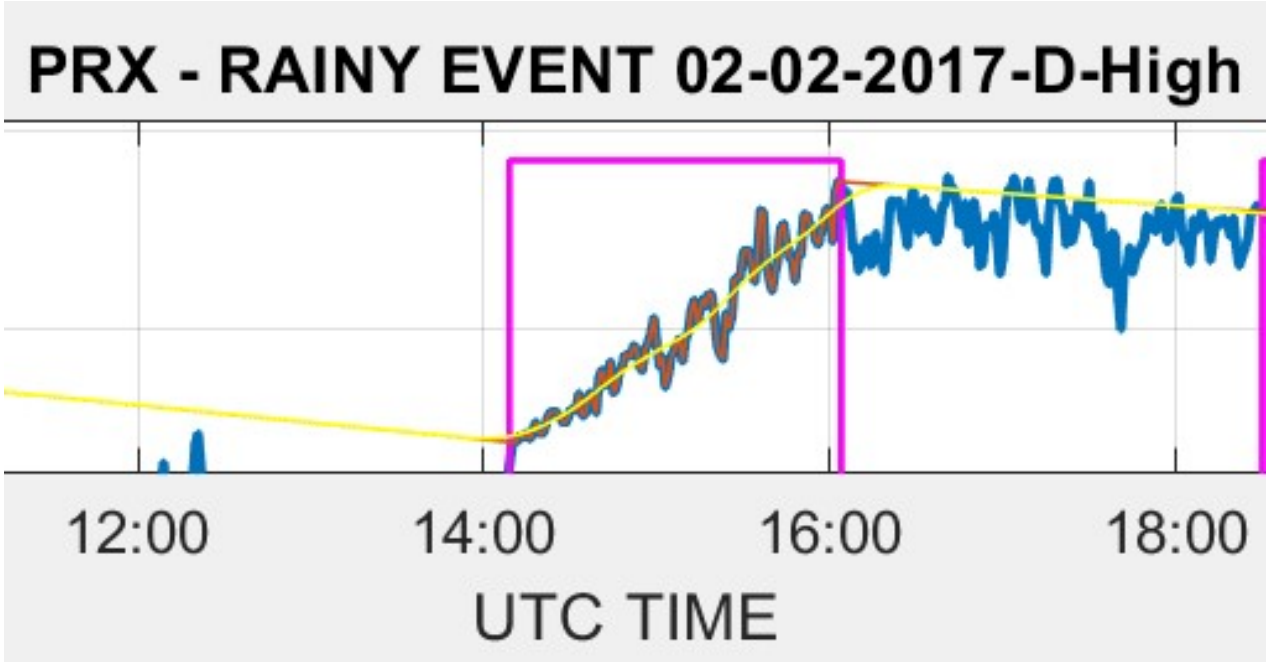

Figure 4-3 Zoom of figure 4-2 in which is observed the drying of the antenna by means the smoother increasing signal

After the precipitation event occurring between 14:00 and 16:00 on 02/02/2017 at D-band-High (156[GHz]), the water accumulated on the antenna gradually dries, which causes a slow increase in PRX back to the values before the rain event.

The solution to this issue was the installation of a hydrophobic shield in February 2018, which helps partially avoiding that the antenna is directly hit by precipitation. Also, (Lorenzo Luini G. R., APRIL 2020), presents a simple model to remove the estimate and remove the wet antenna attenuation A_{WA}:

- For Low frequency – 148[GHz]

$$A *_{WA} = \begin{cases} 0.3528(1 - exp(-1.815\ A_R)), & A_R \leq 1.5\ dB \\ 0.33, & A_R > 1.5\ dB \end{cases}$$

With:

  - A_R : rain attenuation
  - $A *_{WA}$: wet antenna attenuation

- For High frequency – 156[GHz]

$$A *_{WA} = \begin{cases} 0.1068(1 - exp(-4.167\ A_R)), & A_R \leq 0.7\ dB \\ 0.1, & A_R > 0.7\ dB \end{cases}$$

As it is observed, the impact caused by the wet antenna effect is not so strong (0.33dB for 148[GHz] and 0.1dB for 156[GHz]) because part of this effect is mitigated by the rain event.

Finally, it is possible to correct the rain attenuation as follows:

$$A'_R = A_R - A_{WA}$$

From now, the corrected rain attenuation value (A'_R) will be used.

c. RAIN ATTENUATION CCDF

The procedure to calculate the rain attenuation CCDF is similar to the one described above for the rain rate. The result graph is in figure 4-4.

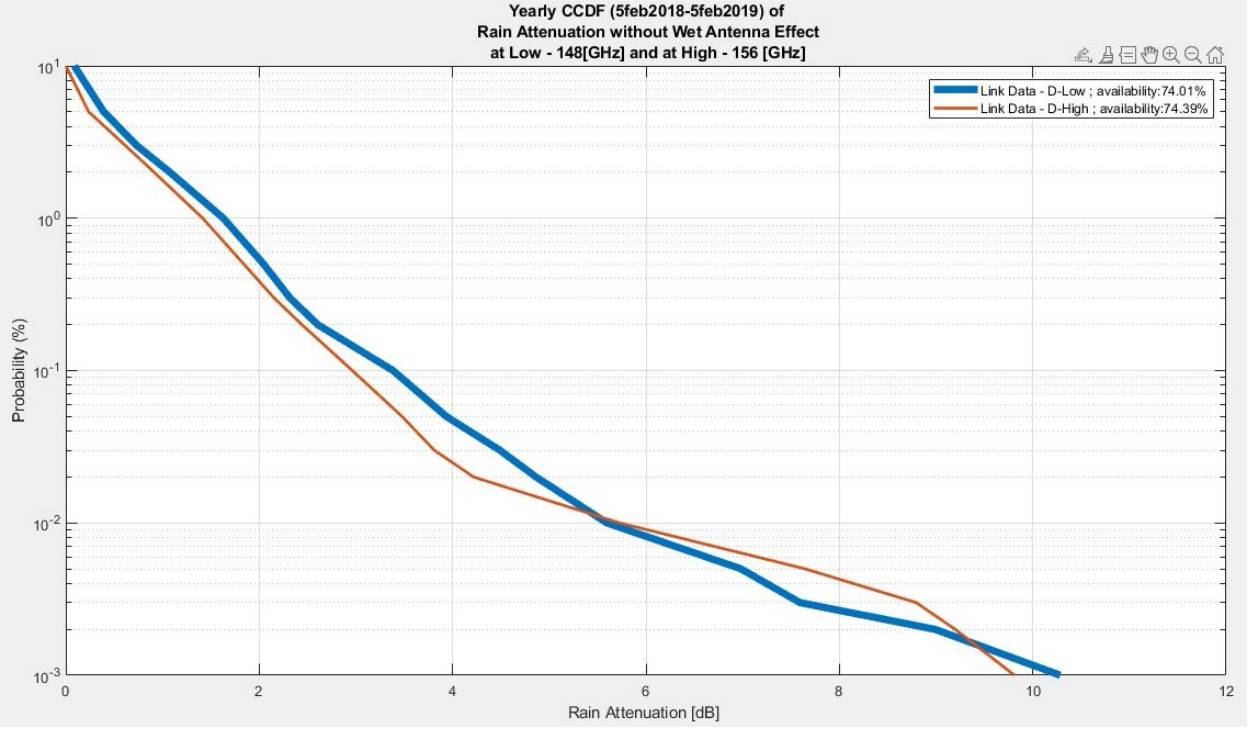

Figure 4-4 Yearly (5feb2018-5feb2019) CCDF of the RAIN ATTENUATION without wet antenna effect at the frequencies 148[GHz] (Low) and 156[GHz] (High).

The results of the rain attenuation CCDF can be seen in tables 4-3 and in figure 4-4 and figure 4-6.

Table 4-3 Results of the rain attenuation without wet antenna effect measured by the link at D-band-low (148[GHz]) from 5 February 2018 to 5 February 2019

$A'_R(dB)$	10.28	8.99	7.59	6.98	5.59	4.86	4.48	3.93
$p(\%)$	0.001	0.002	0.003	0.005	0.01	0.02	0.03	0.05

$A'_R(dB)$	3.38	2.60	2.31	2.04	1.62	1.07	0.73	0.39	0.08
$p(\%)$	0.1	0.2	0.3	0.5	1	2	3	5	10

4.2 Prediction models for rain attenuation

The prediction models considered in this thesis are:

- the recommended model by ITU-R 530.17
- The Lin's model
- The proposed optimised Lin's model

Both Lin-based models rely on a semi-empirical approach, which combines theoretical analyses and measured data (Brussaard, 2013).

4.2.1 Path reduction factor: "r"

As also explained in (ITU-R P.530-17, 2017) (Brussaard, 2013), the rain rate along terrestrial links is not homogeneous, due to the high variability of precipitation. Hence, prediction models must take into account the inhomogeneity for in order to obtain a better estimation of the rain attenuation. This is achieved by means of the dimentionless "path reduction factor" *r*, as a function of the rain rate, whose value typically ranges between 0 and 1, but a higher value can also be verified. The expression of the path reduction factor varies depending on estimation model.

4.2.2 Models

a. Recommended ITU-R 530-17 model

This estimation model is applied in this thesis using as input local and ITU-R derived values.

a.1 Local Inputs

The ITU-R 530-17 recommendation indicates that, at first, the rain rate must be determined for the exceedance probability 0.01%

$$R_{0.01\%} = 77.83\ [mm/h]$$

Then the specific attenuation, calculated exclusively for the same probability value 0.01%, is obtained as:

$$\gamma_{R_{0.01\%}} = kR(0.01\%)^{\alpha}$$

with:

- $\boldsymbol{\alpha}$ and $\boldsymbol{k}$, which are constants that come from (ITU-R P.838-3, 2005), in turn depending on the following parameters and values, see table 4-4:
  1) The elevation angle of the antenna: $\boldsymbol{\theta} = 0[rad]$
  2) Polarisation angle: $\boldsymbol{\tau} = \frac{\pi}{2}\,[rad]$, vertical polarisation.
  3) Operational frequencies used in this experiment:
     - For D-band:
       - Low - 148 [GHz]
       - High - 156 [GHz]

Table 4-4 POWER LAW COEFFICIENTS $\gamma_R = kR^{\alpha}$

	f=148[GHz]	**f=156[GHz]**
$\boldsymbol{\alpha}$	0.6473	0.6445
$\boldsymbol{k}$	1.5852	1.6014

Now, before determining the rain attenuation, *r* is calculated:

$$r = \frac{1}{0.477.d^{0.633}\, R_{(0.01\%)}^{0.073.\alpha}\; f^{0.123} - 10.579\left(1 - exp(-0.024d)\right)}$$

Where:

- f: frequency in [GHz]
- d: path length in [Km]
- $R_{(0.01\%)}$: rain rate at the exceeded probability for 0.01%
- Notice that if the denominator of *r* is lower than 0.4, then, $r = 2.5$.

In this way the effective distance is calculated as follows:

$$d_{eff} = dr$$

Finally, the estimation of the rain attenuation is calculated at the exceeded probability 0.01%, as bellow:

$$\overline{A'(p)_{0.01\%}} = \gamma_{R_{0.01\%}}.d_{eff} = \gamma_{R_{0.01\%}}.d.r$$

In order to obtain the other probabilities (from 0.001% to 10%) for the estimation of the rain attenuation CCDF:

$$\overline{A'(p)_R^{ITU-local-input}}(dB) = C_1.p^{-(C_2+C_3 log_{10}p)}.\overline{A(p)_{0.01\%}}$$

With:

- p: it indicates the probability, by which the correspondence rain attenuation will be calculated
- C_i:
  - $C_1 = (0.07^{C_0})\left[0.12^{(1-C_0)}\right]$
  - $C_2 = 0.855C_0 + 0.546(1 - C_0)$

- $C_3 = 0.139C_0 + 0.043(1 - C_0)$

the results are observable in table 4-5 and figure 4-6.

Table 4-5 Result of the rain attenuation CCDF estimated by using the ITU model with local inputs

$\overline{A'(p)_R^{ITU-local-input}}(dB)$	32.75	29.22	26.82	23.6	19.15	14.92	12.64	10.07
$p(\%)$	0.001	0.002	0.003	0.005	0.01	0.02	0.03	0.05

$\overline{A'(p)_R^{ITU-local-input}}(dB)$	7.13	4.84	3.79	2.73	1.69	1	0.72	0.47	0.25
$p(\%)$	0.1	0.2	0.3	0.5	1	2	3	5	10

a.2 Inputs derived from the ITU-R

In case of absence of information about the rainfall rate, then the Recommendation (ITU-R P.837-7, 2017) should be used. Notice that, the rain rate is obtained from a series of calculations based on digital maps, which were created through a collection of samples provided from many years (1986-1995).

As a result:

$$R_{0.01\%} = 35.3 \left[\frac{mm}{h}\right]$$

The other inputs are the same already shown above.

The results obtained are visible in table 4-6 and figure 4-6.

Table 4-6 Result of the rain attenuation estimation by using the ITU model with derived input

$\overline{A'(p)_R^{ITU-derived-input}}(dB)$	20.52	18.31	16.8	14.79	12	9.34	7.92	6.31
$p(\%)$	0.001	0.002	0.003	0.005	0.01	0.02	0.03	0.05

$\overline{A'(p)_R^{ITU-derived-input}}(dB)$	4.46	3.03	2.37	1.71	1.05	0.62	0.45	0.29	0.15
$p(\%)$	0.1	0.2	0.3	0.5	1	2	3	5	10

b. LIN's Model

This model has a semi-empirical approach, like the one recommended by the ITU-R. First of all, the specific attenuation, based on (ITU-R P.838-3, 2005) and defined as the attenuation measured per km, must be calculated as follow:

$$\gamma_{A_R}^{Lin} = k.R(P)^{\alpha} = \left[\frac{dB}{Km}\right]$$

The parameter $\boldsymbol{k}$ and $\boldsymbol{\alpha}$, are values that come from the ITU.838, as explained in 4.2.2.a.1 and R(P) is extracted from the rain rate CCDF.

For the Lin's model, the path reduction factor is:

$$r = \frac{1}{1 + \frac{d}{d_R}}$$

Where:

- d : path length of the terrestrial link.
- d_R : described as follows:

$$d_R = \frac{2636}{R(P) - 6.2}$$

So:

$$r = \frac{1}{1 + \frac{d}{d_R}}$$

By replacing d_R in r:

$$r = \frac{1}{1 + \frac{d[R(P) - 6.2]}{2636}}$$

$$r = \frac{2636}{2636 + d[R(P) - 6.2]}$$

It means that:

As the rain rate increases, the path reduction factor reduces: if the rain event is more intense, the rain distribution will be more inhomogeneous along the path. The complete expression for the rain attenuation prediction using the Lin's model is:

$$\overline{A'^{Lin}(p)} = \gamma_{A_R}^{Lin} d_{eff} = k.R(P)^{\alpha}.d.r$$

$$\overline{A'^{Lin}(p)} = k.R(P)^{\alpha}.d.\frac{2636}{2636 + d[R(P) - 6.2]}$$

The result obtained are visible in table 4-7 and figure 4-6.

Table 4-7 Result of the rain attenuation estimation by using the LIN model

$\overline{\boldsymbol{A'(p)_R^{Lin}}}(\boldsymbol{dB})$	14.16	12.63	10.63	9.67	8.55	5.89	5.32	4.47
$\boldsymbol{p}(\%)$	0.001	0.002	0.003	0.005	0.01	0.02	0.03	0.05

$\overline{\boldsymbol{A'(p)_R^{Lin}}}(\boldsymbol{dB})$	3.02	2.35	2	1.7	1.3	0.99	0.83	0.61	0.29
$\boldsymbol{p}(\%)$	0.1	0.2	0.3	0.5	1	2	3	5	10

4.3 Optimization of Lin's model and results

The Lin's model is the most promising model to estimate the rain attenuation statistics (see figure 4-6), hence, it has been optimized to increase the accuracy on the estimation. To this aim, the genetic algorithm was applied (MathWorks, 2020).

It is an algorithm used to solve optimization problems and it is based on the law of the strongest, referred to the evolution of the species. It means that if a random number of children is taken to test a solution, only the better ones will survive and will become the reference for the next generation. This cycle is repeated many times to obtain the best children.

Considering a given parameter searching area, random points will be taken to test the objective function to be minimized, for the algorithm to search the best points which give the minimum value of the function.

The algorithm works as in the following example, see figure 4-5.

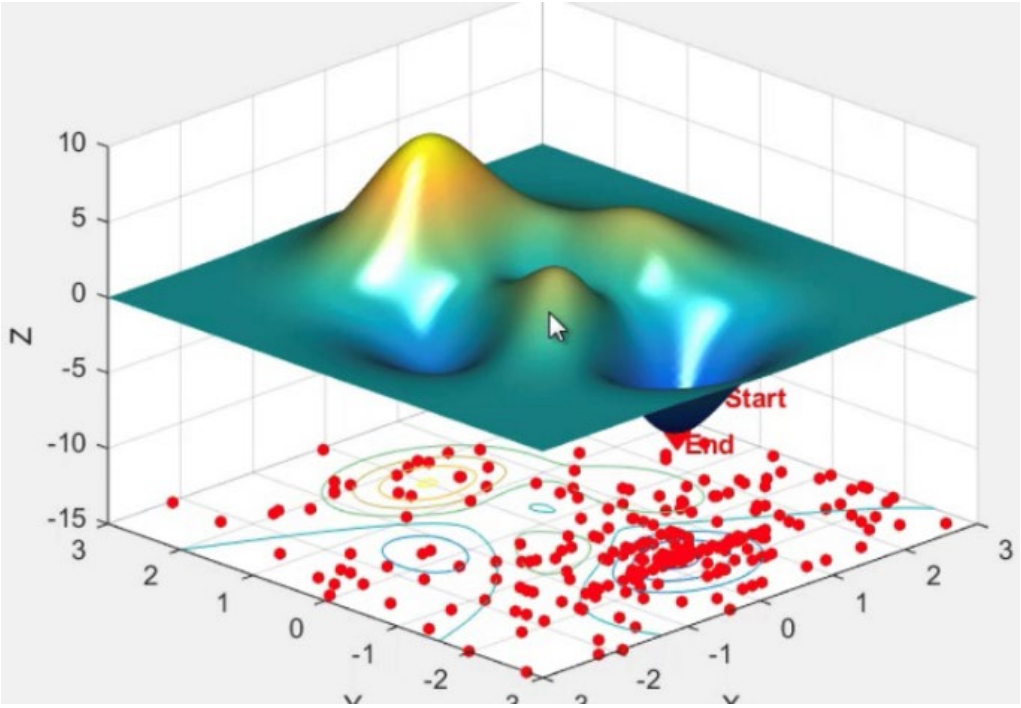

Figure 4-5 Example of the genetic algorithm

By taking again the expression of r (path reduction factor) for the Lin's model,

$$r = \frac{1}{1 + \frac{d}{d_R}}$$

in which, d_R is fined as:

$$d_R = \frac{\mathbf{2636}}{R(P) - \mathbf{6.2}}$$

the coefficients $\mathbf{2636}$ and $\mathbf{6.2}$, will be named as $\boldsymbol{m}$ and $\boldsymbol{n}$, respectively, during the use of the genetic algorithm, which are in fact the parameters to be determined during the optimization process. That algorithm works with a fitness function and with a dedicated script, as explained below.

a. Myfitness function

It is a function that calculates the estimation of the rain attenuation with the standard Lin's model, which then, by means the ITU-R-defined error (Lorenzo Luini S. M., 2020), it is possible to quantity the error as follow:

$$\epsilon(P) = \begin{cases} 100 \left(\frac{A_R(P)}{10}\right)^{0.2} ln\left(\frac{A_P(P)}{A_R(P)}\right), & A_R(P) < 10\ dB \\ 100\ ln\left(\frac{A_P(P)}{A_R(P)}\right), & A_R(P) \geq 10\ dB \end{cases}$$

- $A_R(P)$: reference attenuation extracted from the measured CCDF.
- $A_P(P)$: attenuation extracted from the estimated CCDF.

This operation will be done for the case, D-band, at Low frequency in the period 5 February 2018 to 3 February 2019.

Finally, the average value, standard deviation, and the root mean square (RMS) values are calculated:

$$\mu_\epsilon$$

$$\sigma_\epsilon$$

$$RMS = \sqrt{\mu_\epsilon^2 + \sigma^2}$$

Thus, the fitness function returns the RMS parameter to the calling script, which is the value to be minized.

b. Calling script

This script must limit the area in which the genetic algorithm will elaborate results to minimize the RMS. Then, when the genetic algorithm is running, it

turns out that the examination made on larger areas gives a worst performance, thus, the area has been gradually made smaller until it finds the best couple of values for $\boldsymbol{m}$ and $\boldsymbol{n}$.

The selected limited zone is the following:

$$\mathbf{LB = [-1000 \quad -100]} \qquad (\boldsymbol{x1 = -1000} \qquad \boldsymbol{y1 = -100})$$

$$\mathbf{UB = [1000 \quad 100]} \qquad (\boldsymbol{x2 = 1000} \qquad \boldsymbol{y2 = -100})$$

- LB: Low boundaries
- UB: Up boundaries

After the execution of the genetic algorithm, the search provides the best coefficients for the parameters $\boldsymbol{m}$ and $\boldsymbol{n}$:

$$m = 98.40$$

$$n = -6.1$$

Thus, the new proposed function is:

- The path reduction factor, which is defined as.

$$r = \frac{1}{1 + \frac{d}{d_R}}$$

- Where d_R is defined by the new parameters:

$$d_R = \frac{\mathbf{9840}}{R(P) + \mathbf{6.1}}$$

- Finally, the new path reduction factor with the new optimised parameters is:

$$r = \frac{\mathbf{9840}}{\mathbf{9840} + d[R(P) + \mathbf{6.1}]}$$

So, the new obtained results are in table 4-8. See also figure 4-6.

Table 4-8 Result of the rain attenuation estimation by using the optimised LIN model

$\overline{A'(p)_R^{Opt\ Lin}}(dB)$	9.09	8.59	7.79	7.34	6.75	5.09	4.67	4.02
$p(\%)$	0.001	0.002	0.003	0.005	0.01	0.02	0.03	0.05

$\overline{A'(p)_R^{Opt\ Lin}}(dB)$	2.83	2.23	1.91	1.63	1.26	0.96	0.81	0.6	0.29
$p(\%)$	0.1	0.2	0.3	0.5	1	2	3	5	10

At last, it is possible to compare all resulting data from all models.

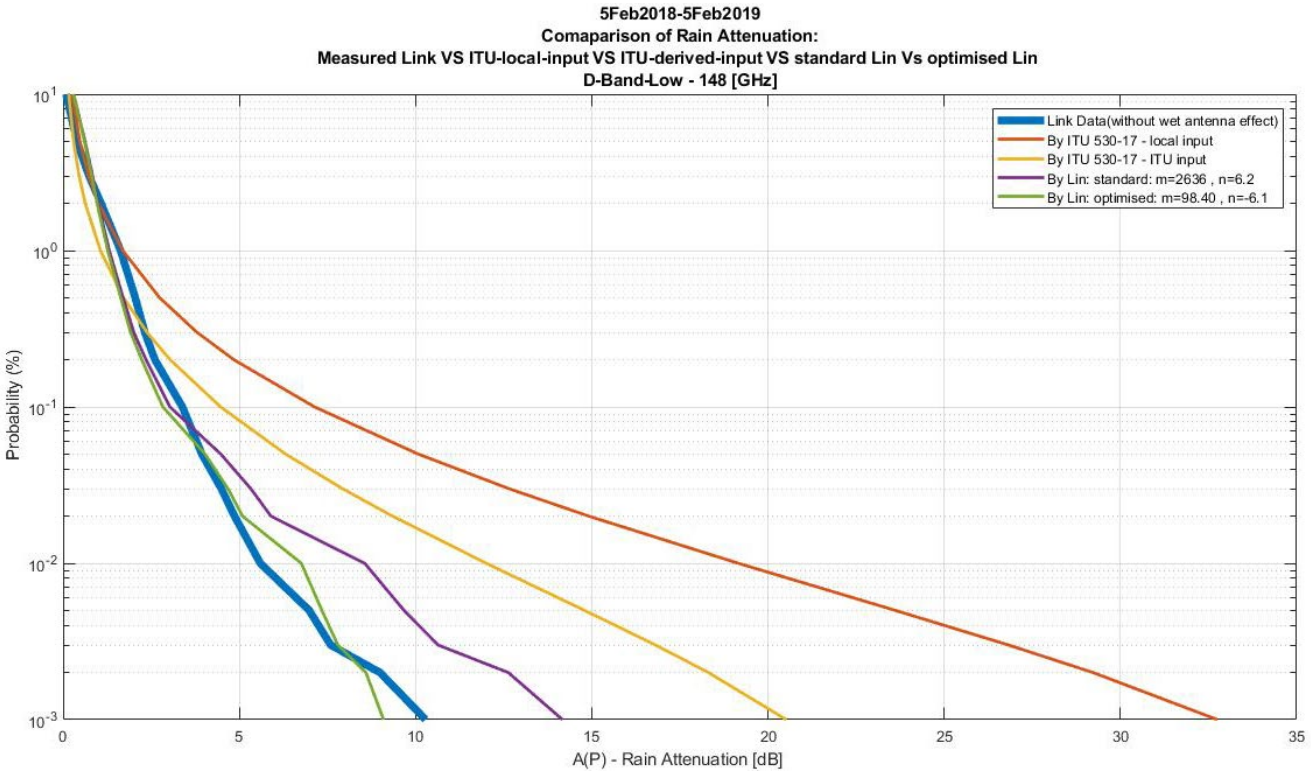

Figure 4-6 Result comparison between the link measured data and ITU model, Lin model and optimized Lin model, at D-band-Low 148[GHz] for the period 5 February 2018 to 5 February 2019.

The recommended ITU model critically overestimates the rain attenuation, while the Lin's model gives better results; the optimized Lin's model provides even better results. The results produced by all the models can be compared with the measured rain attenuation in table 4-9.

Table 4-9 Comparison between the values of rain attenuation measured by the link and all the models; D-band-low (148[GHz]) from 5 February 2018 to 5 February 2019

$p(\%)$	**R(mm/h)**	$A'_R(dB)$	$\overline{A'(p)_R^{ITU-local-input}}$	$\overline{A'(p)_R^{ITU-derived-input}}$	$\overline{A'(p)_R^{Lin}}$	$\overline{A'(p)_R^{Opt\ Lin}}$
0.001	172.70	**10.28**	32.75	20.52	14.16	**9.09**
0.002	143.84	**8.99**	29.22	18.31	12.63	**8.59**
0.003	109.62	**7.59**	26.82	16.8	10.63	**7.79**
0.005	94.34	**6.98**	23.6	14.79	9.67	**7.34**
0.01	77.83	**5.59**	19.15	12	8.55	**6.75**
0.02	43.52	**4.86**	14.92	9.34	5.89	**5.09**
0.03	37.11	**4.48**	12.64	7.92	5.32	**4.67**
0.05	28.28	**3.93**	10.07	6.31	4.47	**4.02**
0.1	15.46	**3.38**	7.13	4.46	3.02	**2.83**
0.2	10.45	**2.60**	4.84	3.03	2.35	**2.23**
0.3	8.16	**2.31**	3.79	2.37	2	**1.91**
0.5	6.32	**2.04**	2.73	1.71	1.7	**1.63**
1	4.21	**1.62**	1.69	1.05	1.3	**1.26**
2	2.75	**1.07**	1	0.62	0.99	**0.96**
3	2.10	**0.73**	0.72	0.45	0.83	**0.81**
5	1.32	**0.39**	0.47	0.29	0.61	**0.6**
10	0.43	**0.08**	0.25	0.15	0.29	**0.29**

The results for the D-band-high, E-band-low and E-band-High are visible in figure 7, figure 8 and figure 9, respectively. The rain attenuation and rain rate CCDFs are extracted from the (Lorenzo Luini G. R., APRIL 2020). As it turns out, the optimized Lin's model offers good results at both E and D bands.

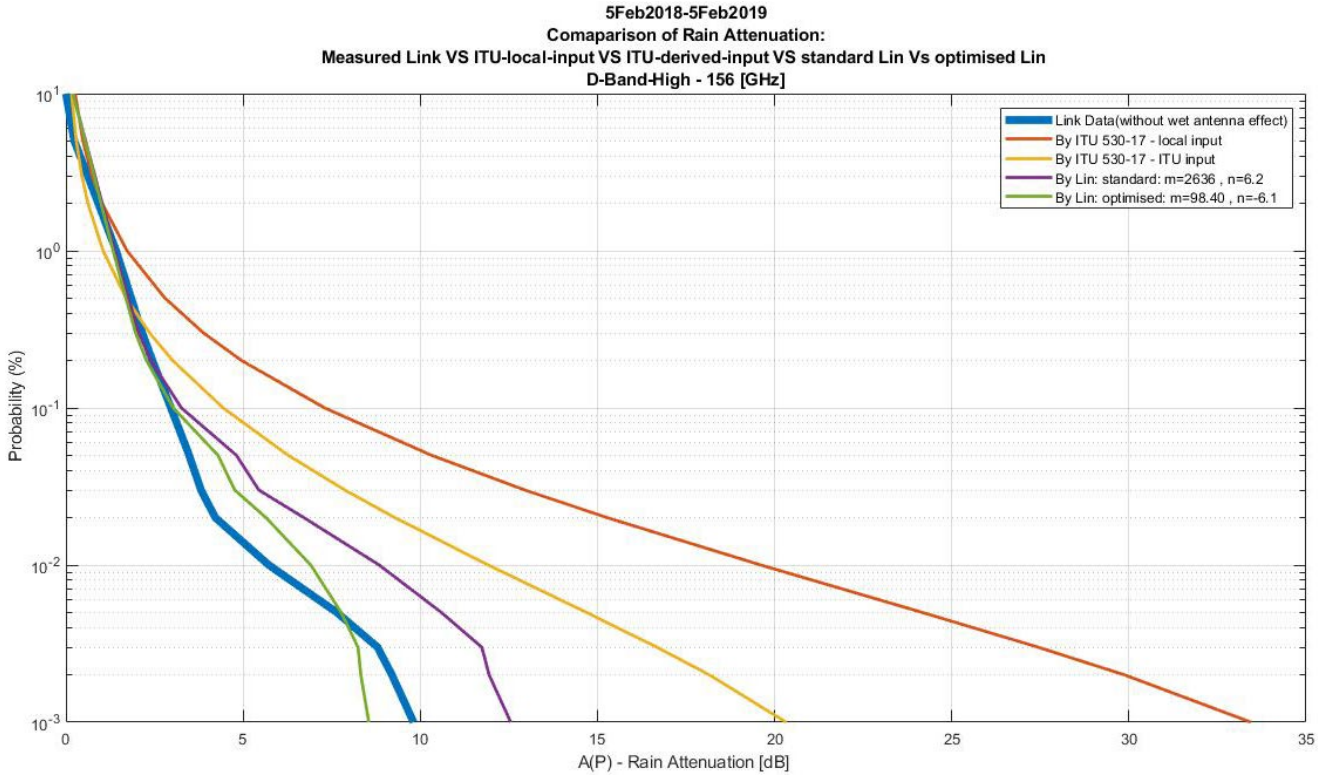

Figure 4-7 Result comparison between the link measured data and ITU model, Lin model and optimized Lin model, at D-band-High-156[GHz] from 5 February 2018 to 5 February 2019.

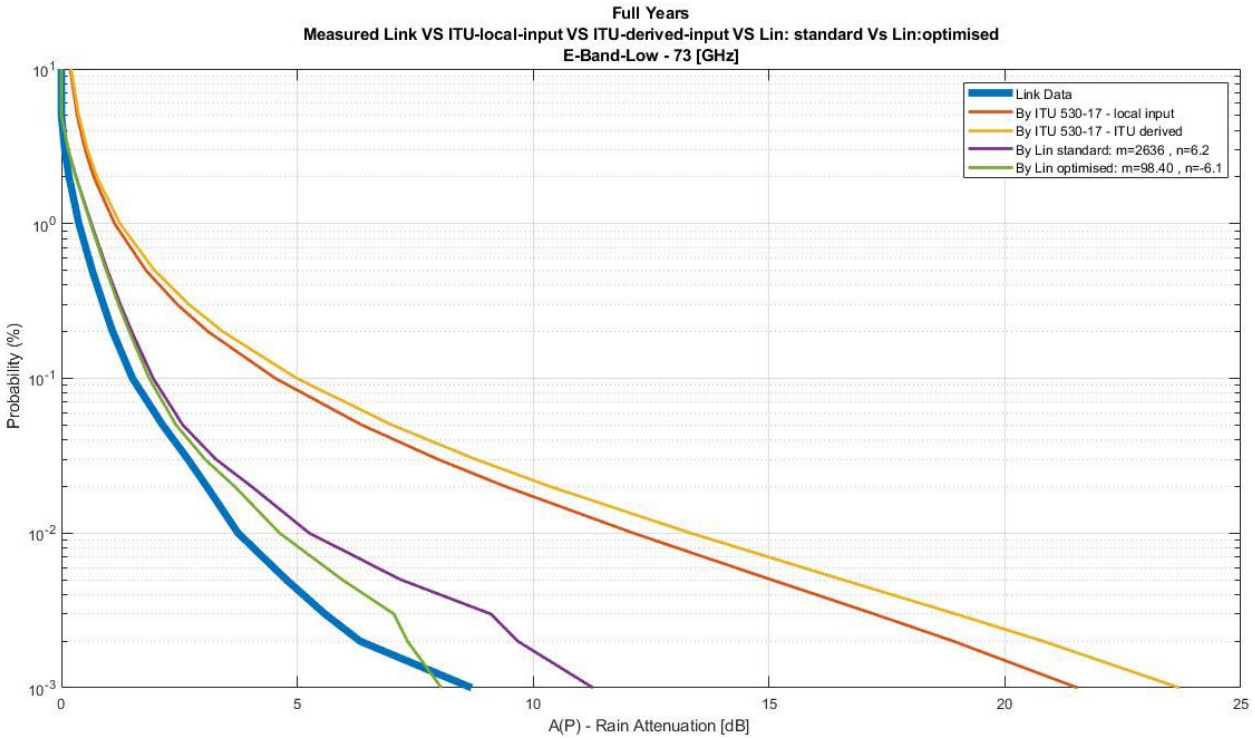

Figure 4-8 Result comparison between the link measured data and ITU model, Lin model and optimized Lin model, at E-band-Low 73[GHz] from 5 February 2018 to 5 February 2019.

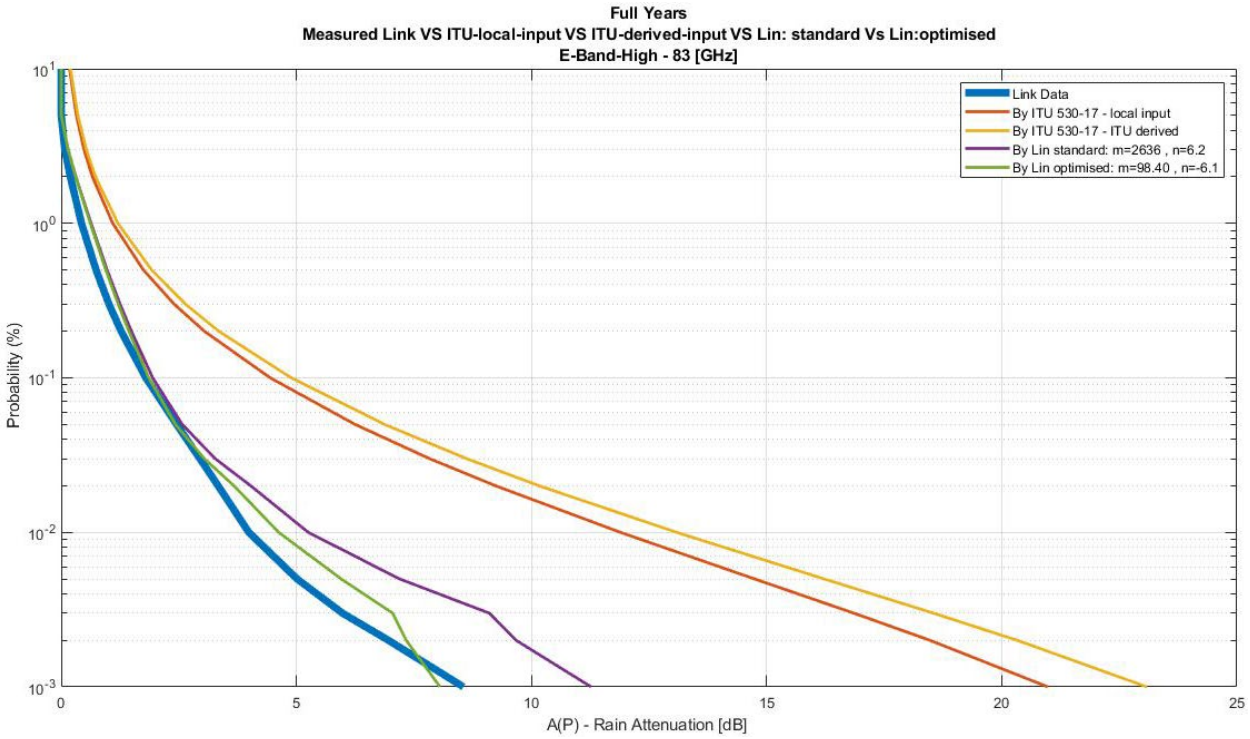

Figure 4-9 Result comparison between the link measured data and ITU model, Lin model and optimized Lin model, at E-band-High 83[GHz] from 5 February 2018 to 5 February 2019.

Conclusions

This thesis presented the results of the experiment conducted in the main campus of Politecnico di Milano, in collaboration with Huawei European Microwave Centre in Milan, to assess the impact of the atmosphere on a 325-m terrestrial link operating at D-band, specifically at 148 and 156 GHz. A full year of concurrent rain rate and rain attenuation data, from February 2018 to February 2019, were elaborated and used in this thesis. The raw data were extracted and elaborated using an ad-hoc MATLAB program, whose results were used to obtain the measured rain attenuation CCDF, to be compared with the statistics estimated by the ITU-model and the Lin model. Results showed a limited accuracy of such models, which prompted us to optimise the Lin model to improve its accuracy.

Results indicate that that the recommended ITU model strongly overestimates the rain attenuation at high frequency and along short links, while Lin's model produces better results. Such a model was optimized using Genetic algorithms, which allows identifying better parameters for the path reduction factor. As a result, the predictions delivered by such a new model are better than those shown by the original Lin model, both at E and D bands.

Bibliography

Brussaard, P. G. (2013). *Handbook on Radiometeorology.* Radiocommunication Bureau.

Cheffena, M. (2010). Measurement Analysis of Amplitude Scintillation for Terrestrial Line-of-Sight Links at 42 GHz. *IEEE Transactions on Antennas and Propagation , vol. 58, no. 6, pp. 2021-2028, June 2010.*

Dr. Lorenzo Luini, P. C. (2018). *THEORETICAL AND EXPERIMENTAL INVESTIGATION OF ATMOSPHERIC EFFECTS ON HIGH FREQUENCY TERRESTRIAL LINKS.* Milano: Poliecnico di Milano.

Emilio Matricciani, M. M. (1996, 03). Relationship between scintillation and rain attenuation at 19.77 GHz. *Radio Science, Volume 31, Number 2*, pp. 273-279.

Fraser, A. B. (2020, 11 23). *USGS Science for a Changing World*. Retrieved from Are Raindrops Shaped Like Teardrops?: https://www.usgs.gov/special-topic/water-science-school/science/are-raindrops-shaped-teardrops?qt-science_center_objects=0#qt-science_center_objects

H. Vasseur, D. V. (1995). *Characterization and Modelling of Turbulence-Induced Scintillation on millimeter-wave Line-of-Sight Links.* Belgium: IEEE Xplore.

ITU. (2020, 11 23). Retrieved from ITU: https://www.itu.int/en/about/Pages/default.aspx

ITU. (2020, 11 23). *ITU-R description*. Retrieved from https://www.itu.int/en/ITU-r/information/Pages/default.aspx

ITU-R P.530-17, R. (2017). *Propagation data and prediction methods required for the design of terrestrial line-of-sight systems.* Geneva: Electronic Publication.

ITU-R P.837-7, R. (2017). *Characteristics of precipitation for propagation modelling.* Geneva: Electronic Publication.

ITU-R P.838-3, R. (2005). *Specific attenuation model for rain for use in prediction methods.*

John F.Federici, J. L. (2016). Review of weather impact on outdoor terahertz wireless communication links. In *Nano Communication Networks* (pp. 13-26). Elsevier.

K. A. Mubarak, A. M. (2009). *Improved Analysis of Spaceborne Radar Signals.* Sharjah: IEEE.

Lorenzo Luini, G. R. (APRIL 2020). *The Impact of Rain on Short E-Band Radio Links.* Milano: IEEE TRANSACTIONS ON ANTENNAS AND PROPAGATION, VOL. 68, NO. 4,.

Lorenzo Luini, S. M. (2020, 07). Enhancement of the Synthetic Storm Technique. *IEEE TRANSACTIONS ON ANTENNAS AND PROPAGATION, VOL. 68, NO. 7*, p. 7.

MathWorks. (2020, 11 23). *Genetic Algorithm*. Retrieved from https://it.mathworks.com/discovery/genetic-algorithm.html

Mukesh Chandra Kestwal Sumit Joshi, L. S. (2014). *Prediction of Rain Attenuation and Impact of Rain in Wave Propagation at Microwave Frequency for Tropical.* Uttarakhand: International Journal of Microwave Science and Technology.

NASA. (2020, 11 23). *Precipitation Education*. Retrieved from The Shape of a Raindrop: https://gpm.nasa.gov/education/articles/shape-of-a-raindrop

Ombra, I. (2014). *Impianto di Raccolta e Trattamento delle Acque Meteoriche, Relazione di Calcolo.* Marsala.

Pedro, J. (n.d.). *Tropospheric Scintillation With Concurrent Rain Attenuation at 50 GHz in Madrid.*

RecensioniOrologi. (2020, 11 23). *Quando cambia l'ora: Cambio ora solare 2020 e ora legale 2021*. Retrieved from https://www.recensioniorologi.it/quando-cambia-l-ora

T.V Omotosho, S. A. (n.d.). *Tropospheric Scintillation and its Impact on Earth-Space Satellite Communication in Nigeria.* Ogun,Lagos.

Wyoming, U. o. (2020, 11 23). *Observations for MILANO LINATE, Italy (LIML)*. Retrieved from http://weather.uwyo.edu/cgi-bin/wyowx.fcgi?TYPE=sflist&DATE=current&HOUR=current&UNITS=A&STATION=LIML

Wyoming, U. o. (2020, 11 23). *University of Wyoming*. Retrieved from University of Wyoming: http://weather.uwyo.edu/